Performance Investigation of Video Streaming over mmWave

Muhammad Abbas Suleiman

Submitted to the
Institute of Graduate Studies and Research
in partial fulfillment of the requirements for the degree of

Master of Science
in
Computer Engineering

Eastern Mediterranean University
May 2021
Gazimağusa, North Cyprus

Approval of the Institute of Graduate Studies and Research

Prof. Dr. Ali Hakan Ulusoy
Director

I certify that this thesis satisfies all the requirements as a thesis for the degree of Master of Science in Computer Engineering.

Prof. Dr. Işık Aybay
Chair, Department of Computer Engineering

We certify that we have read this thesis and that in our opinion it is fully adequate in scope and quality as a thesis for the degree of Master of Science in Computer Engineering.

Assoc. Prof. Dr. Gürcü Öz
Supervisor

Examining Committee

1. Assoc. Prof. Dr. Gürcü Öz

2. Assoc. Prof. Dr. Mohammed Salamah

3. Asst. Prof. Dr. Mehtap Köse Ulukök

ABSTRACT

To provide augmented reality and super-quality video content to consumers, the next generation of multimedia devices demand a higher bit rate of telecommunication networks than today. Most video content is viewed from mobile devices, leading the fifth generation (5G) cellular networks to offer exceptionally high data speeds. Communications at millimeter-wave (mmWave) frequencies are potential enablers here, considering the large amount of available bandwidth that smartphone devices can be assigned. However, the rugged transmission environment at such high frequencies makes it impossible to deliver a trustworthy service due to interference.

This thesis presents the end-to-end 5G system simulation, a simulation model of downlink shared channel (DL-SCH) from MATLAB based on the physical layer, for performance analysis of video streaming over mmWave networks. In the performance investigation, throughput, end-to-end delay, Bit Error Rate (BER) are measured with respect to Signal-to-Noise Ratio (SNR), mmWave carrier frequency and mmWave bandwidth. In addition to this, various Quadrature Amplitude Modulation (QAM) modulation schemes have been used in the simulations. Analytical calculations are also performed to make a comparative analysis on the performance of video streaming over mmWave. In the Long-Term Evolution (LTE) framework Toolbox, the model simulates the channel with a 5G library. The presented investigation has shown the performance of high-quality video at mmWave.

Keywords: mmWave, 5G, Video Streaming, Performance evaluation, Long Term Evaluation

ÖZ

Tüketicilere artırılmış gerçeklik ve süper kaliteli video içeriği sağlamak için, yeni nesil multimedya cihazları, bugün olduğundan daha yüksek bit hızında telekomünikasyon ağları talep ediyor. Çoğu video içeriği mobil cihazlardan izlenir ve beşinci nesil (5G) hücresel ağların olağanüstü yüksek veri hızları sunmasına öncülük eder. Milimetre dalga (mmWave) frekanslarında iletişim, akıllı telefon cihazlarına atanabilecek büyük miktarda mevcut bant genişliği göz önüne alındığında, burada potansiyel kolaylaştırıcılardır. Ancak, bu kadar yüksek frekanslarda sağlam iletim ortamı, parazit nedeniyle güvenilir bir hizmetin verilmesini imkansız hale getirir.

Bu tez, mmWave ağları üzerinden video akışının performans analizi için, MATLAB'da fiziksel katmana dayalı aşağı bağlantı paylaşılan kanalın (DL-SCH) bir simülasyon modeli olan uçtan uca 5G sistem simülasyonunu sunar. Performans araştırmasında, verim, uçtan uca gecikme, Bit Hata Oranı (BER), Sinyal-Gürültü Oranı (SNR), mmWAve taşıyıcı frekansı ve mmWave bant genişliğine göre ölçülür. Buna ek olarak, simülasyonlarda çeşitli Dörtlü Genlik Modülasyon (QAM) modülasyon şemaları kullanılmıştır. mmWave üzerinden video akışının performansı üzerinde karşılaştırmalı bir analiz yapmak için analitik hesaplamalar da yapılmıştır. Uzun Vadeli Evrim (LTE) çerçevesi Araç Kutusu'nda(Toolbox) model, kanalı bir 5G kitaplığı ile simüle eder. Sunulan araştırma, mmWave'de yüksek kaliteli video performansını göstermiştir.

Anahtar Kelimeler: mmWave, 5G, Video Akışı, Performans değerlendirmesi, Uzun Vadeli Değerlendirme (LTE)

DEDICATION

This thesis is dedicated to my family for their sacrifices, love and support.

ACKNOWLEDGMENT

First and foremost, I have to thank Almighty Allah for protecting, guiding, and giving me the strength to go through this thesis successfully.

I would like to wholeheartedly thank my parents, my sisters, and my entire family for their love, support, and inspiration throughout my studies.

I would like to thank my supervisor, Assoc. Prof. Dr. Gürcü Öz for her guidance, support, patience, and understanding, especially for her confidence in me throughout this study.

To all my friends, my colleagues, both at home and around the globe, I say thank you for your understanding, encouragement, inspiration, and for making all the chaos and hard times experienced during this period become fun and memory worth remembering in the future.

Finally, I would like to thank the entire Department of Computer Engineering and Eastern Mediterranean University at large for providing a friendly environment equipped with all the required resources to prepare me and thousands of others for the future.

TABLE OF CONTENTS

LIST OF TABLES

LIST OF FIGURES

LIST OF SYMBOLS AND ABBREVIATIONS

3GPP	Third Generation Partnership Project
4G	Fourth Generation
5G	Fifth Generation
DLSCH	Downlink Share Channel
IP	Internet Protocol
ISI	Inter-Symbol Interference
LTE	Long Term Evolution
MC	Multi-Carrier
MIMO	Multiple Input Multiple Output
mmWave	Millimeter-Wave
MS	Mobile Station
NLoS	None Line of Sight
OFDM	Orthogonal Frequency-Division Multiplexing
PDSCH	Physical Downlink Share Channel
QAM	Quadrature Amplitude Modulation
QoS	Quality of Service
SAE	System Architecture Evolution
SC-FDMA	Single Carrier Frequency Division Multiple Access
SUMO	Single User Multiple Output
UMTS	Universal Mobile Telecommunication System
WiMAX	World-Wide Interoperability for Microwave Access

Chapter 1

INTRODUCTION

The spread of intelligent technology has contributed to an explosive rise in mobile traffic, with the popularity of smartphones and tablets. According to Ramadhan and Nashiruddin, traffic levels on traditional cellular networks are projected to rise 1000 times within the next ten years [1]. We investigated video streaming performance using a 5G millimeter wave (mmWave) transmission to satisfy the customers' needs for high mobile traffic. Many researchers have suggested several new technologies for increasing the capability of existing mobile communication networks based on more than 3GHz frequency bands, such as carrier aggregation, multiple inputs and multiple outputs (MIMO) [2,3]. However, this modern technology cannot fundamentally solve increasing traffic due to restricted bandwidth. Therefore, more bandwidth is needed to improve the communication network. Presently, some experts and industry professionals have started studying the 30-300GHz mmWave band, a radio broadcast band, to create 5G cellular communications networks [4] [5].

Streaming of video resolves a critical aspect of the future generation of cellular systems, and one of its significant high-tech components is mmWave communication. By leveraging the vast volume of the bandwidth available at the frequency, prospective forthcoming mobile systems will provide subscribers with far faster cellular coverage speeds to address the rising demand for fast data rates. Video traffic is the percentage of byte traffic transmitted to their subscribers by smartphone and fixed-line operators.

This form of traffic consumes resources but is proportional to the quality of the service (QoS) provided. In addition, there is vast wastage given that the consumer gives up browsing prematurely in many situations, including lack of interest in the already downloaded video. Some techniques have already been designed to take into account all these drawbacks [4]. Dominant solutions include fast-caching in which the server passes traffic to the client and on-off approaches as efficiently as possible when the client allows the server to pause the transition periodically [5]. The drawbacks encountered in the previous network generations, though viable, can easily be solved with the introduction of the fifth-generation network. The spread loss relative to the typical sub-6 GHz band is much higher, so beamforming performances and advanced network density are required to resolve the path loss possible with the 5G network. However, mmWave communication can be blocked by several materials, including brick and mortar, as well as the human body [6].

1.1 Aim of the Research

In this thesis, we aim to investigate the performance of video streaming over mmWave. For this purpose, we design a system for the end-to-end simulation of the 5G physical layer on MATLAB. The aim is to develop the simulated and analytical performance results of video streaming over mmWave with the simulation of the Downlink Physical layer. A video is used as an input in the simulation and converted to a digital signal initially. Then, we measure Bit Error Rate (BER) against Signal-to-Noise Ratio (SNR), throughput against SNR at various Quadrature Amplitude Modulation (QAM) modulation schemes, and we evaluate the end-to-end delay by varying mmWave bandwidth. MATLAB software was used to measure the system's performance with various modulation schemes on physical layer phenomena.

1.2 Outline

This research is structured as follows. Chapter 1 provides an introduction to streaming videos on mmWave; Chapter 2 discusses literature review, different types of video streaming fifth Generation networks (5G), video compression methods, and related work. Chapter 3 discusses simulation architecture the physical layer transmission. Chapter 4 discusses the simulation setup and results of the simulation, and finally, in Chapter 5, we discuss the results, draw a conclusion and give prospects of future work.

Chapter 2

LITERATURE REVIEW

In this section we look at the core structure of video streaming in order to we understand the big picture of video streaming service control over wireless links.

2.1 Video Streaming Systems Overview

Since our emphasis has been on 5G mmWave, we explain the various level view of a point on video streaming systems from the perspective of the network architecture layers, as shown in Figure 2.1.

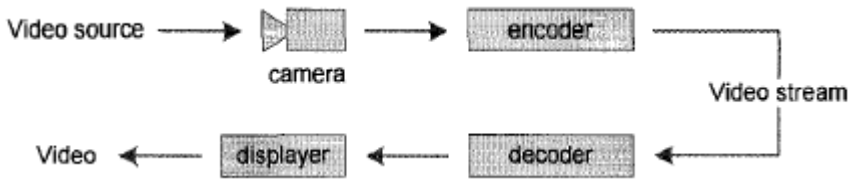

(a) Video source view

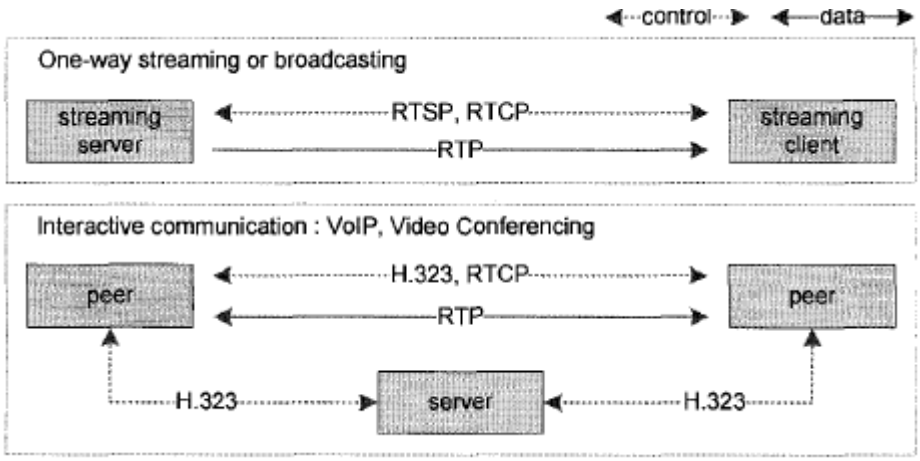

(b) Application-level view

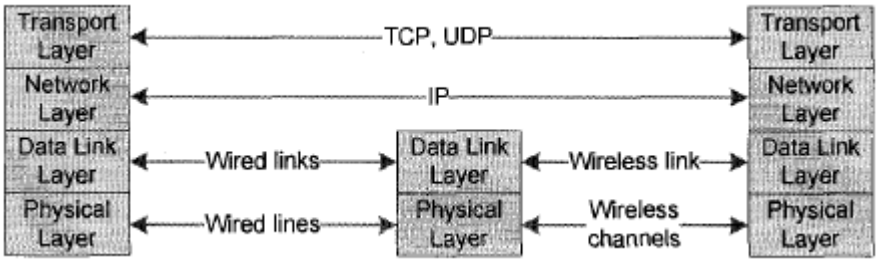

(c) Network-level view

Figure 2.1: Video streaming system overview[7]

The video source has busty features immediately after compression, which relates to the timing of human eye recognition. In other words, video streams have independent image data every half second play a seamless video by default [7]. Intermediate image data between two consecutive independent image data frames refer to each other or adjacent independent image data frames bi-directionally.

Intermediate image data are relatively small in size with respect to the independent image data. These bursting characteristics make it necessary to support variable bit rate data in the network. However, the Internet Protocol (IP) networks are often described as 'best effort' networks that do not benefit from variable bit rate data. So, the current video encoders have 2-level rate matching modules to create a consistent bit rate stream of video. The bit rate is not perfect but better than the previous bit rate variable streams.

2.1.1 Streaming Application

The video stream is used for interactive video and streaming media. H.323[8] provides independent network/platform/application management and bandwidth management for interactive video applications, such as Video or Voice over Internet Protocol (VoIP). Video broadcasting scenario is quite different. The Real-Time Streaming

Protocol (RTSP) [5] provides the functionality of Video Cassette Recorder (VCR) such as play, forward, reward, stop, etc. The real-time transport protocol (RTP [9]) encapsulates video data to use various controls in real-time. In order to increase sending rate controllability, the video stream application uses a small packet to transfer the video stream.

2.1.2 Network Consideration

The video stream has time and rate constraints. Unless a packet arrives within a specific time, it cannot be used even if it arrives a little later. The network must therefore be continuous~~ly~~ and timely to feed video stream data to the video player decoder. However, the decoder input buffer can compensate for a non-severe delay. Also, the buffer size is proportional to the delay of playback and demands a memory resource. Most streaming applications use User Datagram Protocol (UDP) [10] instead of TCP [8] to reduce transmission delays. Even though TCP is the dominant protocol for the transport layer, it is much extremely tricky than UDP. For instance, TCP has a retransmission system that leads to variance in delay. UDP, on the other hand, is simple and does not retransmit. The application must, however, be responsible for controlling its rate and handling lost information. Recently, the Datagram Congestion Control Protocol (DCCP) [11] was introduced as a simple and rate-controlled transport control protocol. The video stream rate constraints accept a most diminutive continuous reproduction. Current sophisticated streaming technologies enable rate-scalable encoding. The sending rate can be adjusted with the corresponding rate-encoded stream based on the observed packet loss rate. Both of these limitations are directly linked to the Quality of service (QoS) issue and is still not sufficient on the existing internet. QoS support is most desirable in building dedicated networks.

2.2 Streaming of Video

Video streaming over networks is measured to be the most motivating application. Streaming Stored Audio and Video, Streaming Live Audio and Video, and Real-Time Interactive Audio and Video are the significant types of streaming media distribution methods. Figure 2.2 shows the general structure for video streaming. Wide bandwidth, reliable routing protocols and content distribution procedures are essential for this application to ensure smooth receiver video playback [12,13].

A stream of stored audio/video records is compressed and stored on the computer in the first group. Then, the recipient downloads the files via the internet. Hence, they are usually called audio/video-on-demand. Secondly, stream lives audio/video applies to broadcast radio and TV shows over the internet. Finally, interactive audio/video is used for interactive audio/video applications also in the third group, i.e., a perfect example of this technology is Internet telephony and Web teleconferencing [14].

2.2.1 Architecture of Video Streaming

In the video streaming architecture (see Figure 2.2), the video and audio files are compressed and then stored over storage devices by video and audio compression algorithms.

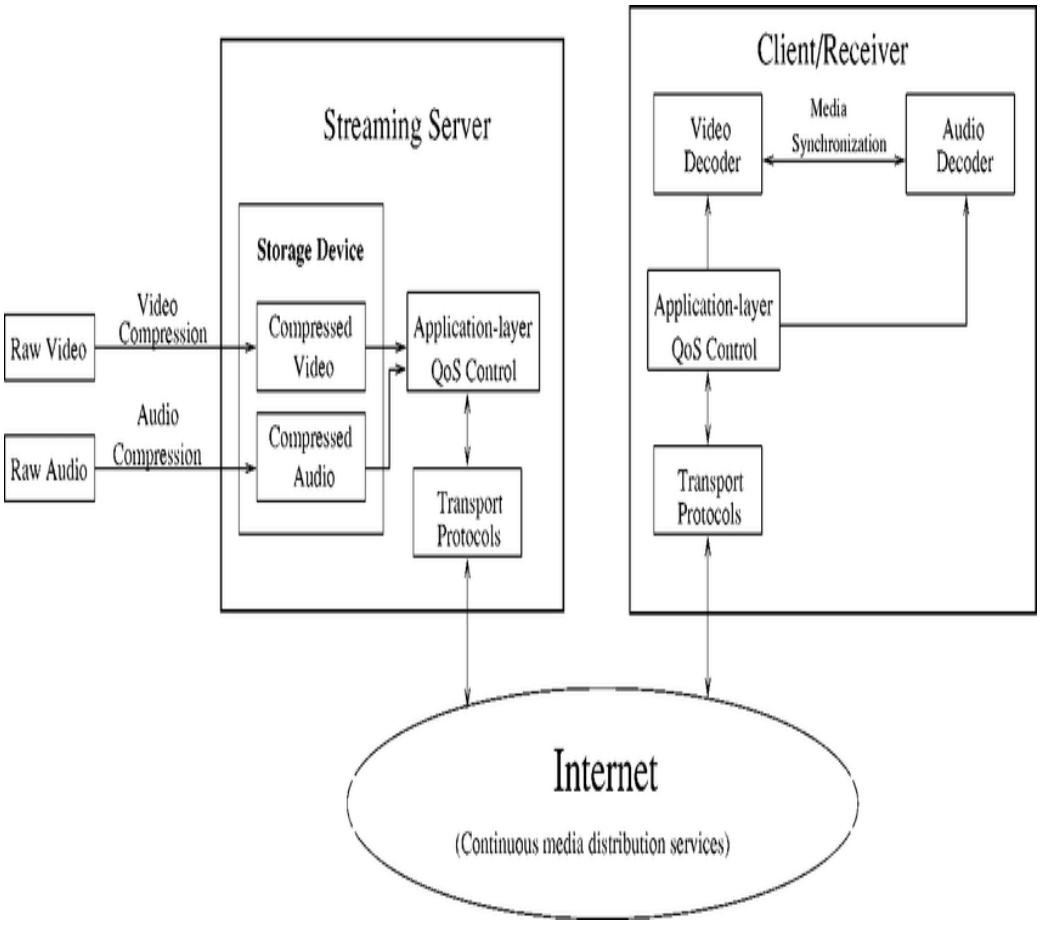

Figure 2.2: Video streaming architecture. [5]

The streaming server receives video/audio compressed data from the storage devices on the user's request, then modifies the QoS video/audio bitstream application-layer QoS control module to satisfy the network state and the QoS specifications. The transport protocols merge the encoded bitstreams and upload the video/audio packages to the internet as they are adapted. Because of congestion, packets can be skipped or delayed over the internet. In order to promote video and audio delivery reliable video and audio delivery reliably, consistent media storage mechanisms (e.g., caching) are implemented on the internet. For packets sent to the receiver successfully, they first pass over transmission layers and process the application layer before decoding to the video/audio decoder. In addition, mechanisms of channel synchronization are necessary for video-audio presentations to be synchronized [5].

2.2.2 Streaming Over LTE

A critical issue in the field of wireless communication is the advancement of mobile network technology. The fourth (4G) Generation reliability was created as a result of this innovation. Within 4G, the LTE was introduced to apply radio access technologies to fixed audio, video, and data services [15]. Due to LTE applications, LTE technology has become popular. LTE was structured in the 3rd Generation Partnership Project (3GPP) to improve data transmission. However, the fundamental concept of such a technology was just too inspire and motivate streaming of multimedia using LTE to provide high-performance radio-access technology [16].

One of the primary reasons for LTE's evolution is developing IP-based services to people on mobile devices with excellent QoS [17]. 3G networks have already offered some technologies, but providing HD video streaming, interactive video games and other multimedia services without reducing service quality is a big challenge. Video streaming over the mobile internet is the most common of these multimedia services. In order to preserve the consistency of the service and the efficiency of the application, it is necessary to be mindful of customer experience as data rates and resources are on the rise.

Quality of Experience (QoE) is defined as understanding the customer's actual performance to ensure those services meet customer expectations and requirements. Understanding user experience is very critical for the network operators in managing the QoS of the network. QoE measurements are made at the point of delivery directly from the subscriber's smartphone or PC. QoE measurements deal with how well applications (Video streaming, VoIP and Web browsing) work in the subscriber's hands.

2.2.3 Video Streaming Over the Internet

Media streaming systems are different from file-sharing systems [18] in which the client has to download the entire file before using it. Real-time multimedia, as the name implies, has time constraints. For example, audio and video data must be played on an ongoing basis. If the data does not arrive in time, the playout cycle will stop and this is frustrating to human ears and eyes.

Real-time transmission of live video or video storage is the predominant part of real-time multimedia. Researchers in [19] dealt with video streaming, which relates to transferring data stored in real-time. There are two modes of transmission of stored video over the internet: download mode and streaming mode (i.e., video streaming). In streaming mode, video content does not need to be entirely downloaded but is played as parts of the content are processed and decoded. Due to its real-time nature, video streaming typically requires broader bandwidth or may results in delay and loss. However, the current best-effort internet does not offer any QoS guarantees to stream video over the internet. Also, it is difficult for multicast users to fully accept multicast video while at the same time providing service flexibility to satisfy a wide range of QoS criteria. Therefore, designing systems and protocols for video streaming on the internet also faces many challenges.

2.2.4 Streaming Stored Audio/Video

Streaming stored video can be conducted by downloading compressed media files from servers in the unicast mode (on-demand media service). The client (user) downloads the desired media file, uncompresses it, and then plays it. It is possible to pause, rewind and fast-forward the playout. The latency can be pretty significant from sending a request to a server (a few seconds or dozens of seconds). In general, the

client can begin the playout of the requested file without waiting for its complete download, concurrently with the process of downloading. The displayed part of the downloaded file may be removed from the memory if it is not required for rewinding. It could be different from retrieving other types of files from the server if downloaded [5, 20].

2.2.5 Streaming of Live Audio/Video

Audio and video broadcast is equal to audio or video streaming through radio and TV. The stations are reporting on the phone, not on the radio. Some similarities exist between downloading and live streaming audio and video; they are both prone to delays, and neither will they consider retransmission. However, a gap remains. In the first application, the contact is unicast and on request, while in the second, the communication is live and multicast. A live stream is suitable for IP multicast networks and the use of UDP and RTP protocols. For instance: Online Radio, Internet TV (ITV), and Internet Television Protocol. (IPTV) [21]

2.2.6 Real-time Interactive Audio/Video

In [22], real-time virtual audio/video, individuals communicate in real-time. The Internet phone or Voice over IP is an example of this form of usage. Another indication of how to communicate both physically and verbally is video conferencing.

They explore such real-time audio and video communication capabilities when discussing protocols used in this class of applications.

2.3 Phases of Video Downloading

The phases of video downloading techniques [5] were identified and discussed in this section.

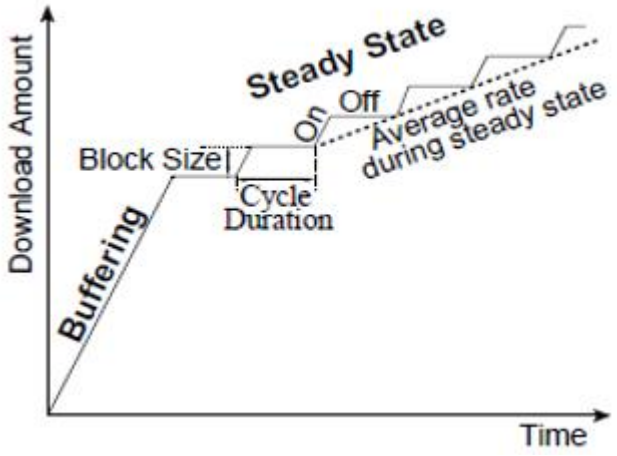

Figure 2.3: Phases of video download [5]

The video content is broadcast in two stages during a regular streaming session: buffering period, then followed by steady-state phase. Video loading continues with a buffering phase followed by a steady-state streaming phase. The ON-OFF periods in the steady-state process are used to minimize the downloading rate.

The available end-to-end bandwidth constrains the data transmission speed during the buffering process. The line's slope during the buffering process in Figure 2.3 is the available end-to-end bandwidth. The video player begins playback when a sufficient amount of data is available in its buffer. Video playback does not wait for the buffering phase to end.

The average download rate is slightly higher than the rate of video encoding in the steady-state phase. At least one accumulation ratio is ideal because a less than one accumulation ratio will cause the video playback to be interrupted due to empty buffers [5, 23].

By constantly uploading one block of video content, the average download speed in the steady-state phase is reached. These periodic transfers produce ON-OFF periods. During each ON cycle, the data block is transferred to the available end-to-end bandwidth that TCP can use during OFF periods when the TCP connection is idle. The ON download slope shown in Figure 2.3 is the end-to-end bandwidth available by naming the block size of the amount of data transmitted in one cycle. The buffer process ensures that the player has adequate data during video playback to compensate for the bandwidth variation. The decreased transmitting rate means that the volume of video content does not overload the video player during the buffering process while retaining or increasing buffered data [24]. The decreased data transfer rate is essential for mobile devices that cannot store the entire video. It is also assumed that the decreased rate lowers load at the steady-state stage of the streaming infrastructure. The reduction in load raises the number of videos that can be concurrently accessed [25].

2.4 Video Streaming vs. Video Teleconferencing

There are two primary data traffic methods, interactive and broadcast video, depending on the device case scenario. Although video streaming (e.g., Netflix and YouTube) allows for modest pausing (within few seconds) before the replay starts, immersive videos such as video teleconferencing (e.g., Facetime [23] and WebRTC [24]) are also interactively speaking (i.e., FAQ). Videos are also a very significant differential element in the quality of the experience and quality of service. Any frame should be transmitted and decoded in a limited time (less than a few hundred milliseconds) and real-time images.

2.5 Video Compression

Compression is a method to produce an image in a compressed digital file. The language code used to refer to image, video stream, or audio signal, is data

compression, bandwidth suppression, and signal compression. The general problem of compression is to minimize the bit-rate of a digital representation. The picture is suitable for many uses. Video and audio signals in the compressed format are available. Many of these implementations were not possible without compression. Video compression is used to significantly reduce the extreme amount of bandwidth/space needed to encode or transmit files. There is a high degree of redundancy in video data represented in two forms: spatial redundancy and temporal redundancy. Several pixels in a frame are frequently repeated or very close to other neighboring pixels; this is referred to as spatial redundancy. It refers to the correlation of adjacent pixels within the same frame. Consecutive frames in a video are often essentially identical. Temporal redundancy refers to the similarity of successive frames [25, 26].

Steps in video compression

- Step 1. Using the Motion Estimation and Compensation (ME & MC) to minimize temporary redundancy. If the current frame is the first frame, the encoder cannot perform ME & MC because the first frame has no relation to the previous neighboring frame. It is called intra-coding. If the current frame is not the first frame, the encoder executes ME & MC to minimize redundancy. As a result, it obtains a frame difference between the existing and adjacent frames.
- Step 2. To minimize spatial redundancy, add discreet cosine transform (DCT) to a frame or difference frame. The frequency of DCT coefficients is the product obtained in this step.

- Step 3. Quantize the DCT coefficients. It decreases data quality and results in a lack of video signal. This stage is responsible for the vast majority of compression seen in the video encoding process at the risk of minimal visual degradation.
- Step 4. Zigzag scan and entropy code quantified coefficients to minimize bits further.
- After implementing the above main steps, the output of the video encoder is a compressed binary bit stream that is appropriate for storage or transmission. Figure 2.4 below describes the generic video coding scheme.

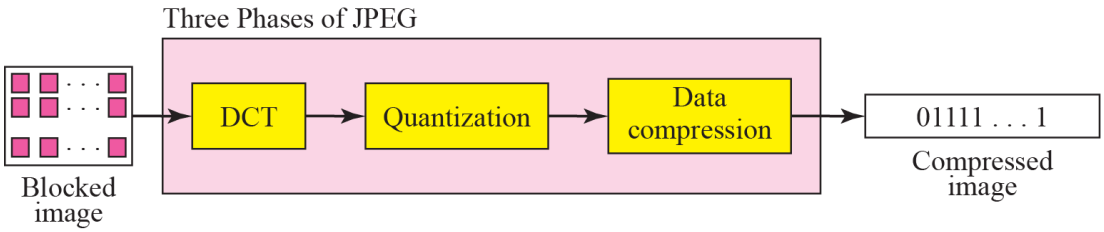

Figure 2.4: Processes of video compression [17]

2.6 Millimeter-Wave (mmWave)

The 5G cellular technology uses the mmWave frequency as carrier frequency to increase wireless network bandwidth. The mmWave is ideal for all wavelengths of 1 - 10 mm and frequency bands from 30 to 300 GHz. In general, submillimeter waves have a radio frequency from 10 to 30 GHz with the same propagating characteristics as mmWave. Unlike mobile networks of 4G LTE, mmWave telecommunications like 5G and IEEE 802.11ad significantly upgrade cellular network capability and will use a larger spectrum than the present 4G LTE [6].

What is precisely 5G? 5G is the foundation of virtual reality Internet of Things (IoT), autonomous driving. There is five brand-new technology immerge as a foundation of 5G (1) mmWave (2) small cell network (3) massive MIMO (4) beamforming (5) full-duplex.

mmWave: Smartphones and other technologies in our home are particular on the radio frequency spectrum, typically under 6 GHz. These frequencies have started getting more crowded. Chores only can squeeze so many bits of data on the same amount of frequency spectrum. As more devices come online, slower and drought connection are seen; the solution is to open a new spectrum which is known as mmWave these range from 30-300GHz [3]. This spectrum has never been used by other devices and it can bring more bandwidth to everyone. The problem is that it cannot pass through a building and other obstacle and tend to be absorbed by plants and the rain. In order to overcome this problem, small cell network technology should be taken into consideration.

Small cell network: Today's cellular network allows the higher tower to broadcast their signals to long distances, but the remaining higher frequency faces serious difficulty traveling through obstacles. This means a cellular moving behind an obstacle can lose its signals. A small cell network would solve this problem by using 1000 base stations, which must be closer to each other, commonly used in the city. As the signal move behind the obstacle will automatically switch base station with better range of device that allows the user not to lose connection [10].

Massive MIMO: Massive multiple inputs multiple output**s** 4G base station has dozens of ports that handle all cellular traffic, but MIMO base station can support hundred

base stations, increasing the network's capacity by a factor of 22 or more [2]. However, MIMO also comes with its complications. For example, today's cellular network broadcast information to every direction at ones and all these crossings of the signal causes serious interference which addressed by beamforming technology.

Beamforming: Beamforming is like a traffic system in a cellular signal, instate of broadcasting in every direction. It allows a base station to send a focused stream of data to a specific user. This precision prevents interference and gives more efficiency, which means the station can handle more incoming and outgoing data at once.

As reported by previous work [9], the benefits of mmWave communication can be described as follows:

- Since mmWave comprises unused primarily radio frequencies, mmWave communication can take up a broader spectrum without radio interference from various radio systems.
- Availability of broad bandwidth will lead to more excellent network link capability without the implementation of multi-level modulation.
- The shorter wavelength allows an antenna with small-sized features, lightweight, better directivity, and higher gain to be understood. This antenna can be installed effectively and efficiently, especially on mobile devices such as smartphones.

Also, in [6], the problems of mmWave communications have been addressed, and thus the problems can be defined as follows:

- The failure to radio propagation is growing, especially related to frequency bands of below 10 GHz. In general, precipitation particles, including rainfall, are gradually attenuated.
- The spreading distance is therefore reduced. However, the spectrum is narrower with an increase in wavelength and mmWave spread too straight, meaning that there is increased spread loss due to barriers and often interference fades.

2.6.1 Transition in 4G to 5G Mobile Network

5G is a new digital system for transforming bytes - data units - over the air. It uses a 5G New Radio (NR) interface and other new technologies that utilize much higher radio frequencies to transfer exponentially more data over the air. This is for faster speeds, reduced congestion, and lower latency, which gives an indication the delay before a data transfer begins following an instruction.

The mobile communication technologies are tracked back to various generations 1G, 2G, 3G and 4G. 1G, which started in 1980, stands for the first generation of wireless telecommunications popularly known as cellular phones, in which analog radio signals are used. In 1991 2G (Second Generation) wireless telephone technology started using digital mobile systems [15]. The second-generation mobile technologies provide low bandwidth services, which are suitable for voice traffic. The packet data over cellular systems started with the introduction of GPRS (General Packet Radio Services) in GSM (Global System for Mobile Communications). With the introduction of 3G technology, network operators can provide better and more advanced services like video calls and mobile broadband services.

All IP Network (AIPN) is designed to satisfy cellular connectivity demand by developing a 3GPP system. It is a combination application suitable for various forms of radio access technologies. Firstly, AIPN emphasizes package-switched technology enhancements. However, today it offers uninterrupted growth and optimization both in execution and expense. The critical advantage of AlPN architecture is that multiple access mechanisms are gathered, have reduced costs, fast for global networking, increased process satisfaction, and reduced latency.

On the other hand, some difficult problems have arisen with the aid of the IP: the data flow is getting more transparent. The internet is opening up to all sorts of malware and criminals, which implies it is not only available to developers. Moreover, there may be several varieties of a base station in 5G networks comprising Device to Device (D2D), User Densification Network (UDN), and large classical MIMO macros. These multiple base stations also control horizontally rather than collectively in 4G networks and follow cellular networks that are powerful and sensitive.

Contrary to 4G, the 5G station would potentially provide a modulation plan, radios, and an internet-based new error monitor planner. Evolution is shown across consumer stations as a concentration of 5G cell networks. These stations can utilize wireless systems simultaneously, and the station will be able to integrate different flows of different technologies. Each 5G network can handle consumer mobility while the terminal provides the final option for specific services between different wireless mobile access networks. This choice depends on turning on the mobile phone's intelligent middleware [2, 4, 15].

2.7 Related Work

The video service is among the most challenging multimedia services; it generates an immense volume of data that must be easily transmitted and processed; without highly efficient compression systems will be impossible/infectious. In the uncompressed video, the standard video encoding (like H.264 and VP8) leverages spatial and temporal redundancy to achieve a decent compressive ratio, leaving the compressed video susceptible to transmission errors. The video frame compressed and encoded cannot decode or be played before receiving all or more packages on the receiver side. Packet errors are subsequently caused by retransmission on the receiver side, and constituent packets are received in time. As a consequence, packet losses are due to transmission errors [27,28]. Many researchers are working on improving video streaming over the mmWave network with different approaches.

In [1], Peer-to-Peer (P2P) live video streaming systems in the flash crowd were discussed, which has recently received substantial attention, with commercial deployment gaining popularity on the internet. The result obtained helps to ascertain the importance of prioritizing multimedia traffic to achieve better QoS performance in low and high network loads. Unfortunately, although this is somehow related to this thesis work, it does not work on mmWave.

In [2], simulations were conducted to investigate the reliability of video streaming with multiple connectivities and video encoding on the mmWave link. In addition, the authors tried to show that communication can allow high data rates at a high frequency, which are needed to support the source rate of high-quality videos. A novel simulation framework that combines the module ns-3 mmWave with a realistic application layer

based on real H.264 video traces was used to evaluate the proposed solution. The results obtained showed an improvement in typical video streaming performance. Such as Network Abstraction Layer Units (NALU) and PSNR at the application layer and the importance of introducing multiple connectivity and signify that network coding can reduce NALU loss and increase PSNR in particularly with mmWave.

In [8], TCP throughput characteristics over a 5G mmWave network were investigated in an indoor train station. The research was conducted on 5G and throughput performances were evaluated in an indoor train station by considering the effect of an NLOS environment caused by blockage of human bodies. The results obtained show an improvement in the robustness of TCP transmission in a high-RTT and high-packet loss environment (e.g., an NLOS environment).

In [11], simulations were conducted on a dynamic QoE model to evaluate 5G mmWave video streaming. The simulation was built in an end-to-end streaming system with ns-3 simulation tools. Furthermore, the Evalvid tool was used to obtain the video transmission from the network of mmWave. The results obtained show an improvement in the performance PSNR value by reconstructing the video and comparing the raw video. Finally, the formula of non-linear regression and exponential function was used to map the QoS parameters to the MOS value. In addition to that, video estimation QoE on a 5G millimeter-wave scenario was also obtained.

In [4], the authors proposed a distributed solution to reduce the playback latency of P2P live streaming services using Content Delivery Network (CDN) servers. The results obtained show an improvement in the proposed method that can reduce the playback latency by limiting the distance from the content server. Also, the proposed

solution constructs a data distribution graph with a shorter average distance than the previous random membership method without heavy server traffic load.

In [7], a performance comparison of dual connectivity and hard handover for LTE-5G was performed. It was observed that mmWave frequencies suffer from very high isotropic path loss, resulting in cells with a much smaller coverage area than current LTE microcells. High directionality techniques were used to improve signal quality and extend coverage area, along with a high-density deployment of mmWave base stations (BS). The simulation and modeling are based on the ns–3 and use the 5G mmWave protocol stack developed by New York University (NYU) and the LTE. In the research, two possible ways to integrate 5G and LTE networks were investigated to improve the reliability of next-generation mobile networks.

The authors in [10] focused on investigating the performance of transportation layer routing protocols (UDP and TCP) considered the core protocols of the Internet protocol suite. Therefore, the behaviors of these routing protocols with different network metrics and scenarios were simulated. Furthermore, Network Simulator version 2.35 (ns-2) is utilized to analyze and evaluate the performance for both TCP and UDP protocols by varying the packet size and the bandwidth.

In [22], simulations were conducted on the downlink subcarrier allocation scheme of the LTE network to investigate the efficient utilization of the available resources in the LTE network at the downlink layer. The results obtained show an improvement in the performance of VoIP applications when each traffic is grouped into different classes.

Also, [29] discusses how high-speed optical signals transmission and reception by using 4-pulsed amplitude modulation (4-PAM) and demodulation in 10 Gbps passive optical access systems with different bandwidth Optical Bessel Filter (OBF). The simulation results prove that the BER performance achieves the optimal when the OBF bandwidth increases and the BER performance can be achieved for the downlink.

In [30] authors investigated the performance of MIMO-OFDM technology using two different transmission channels; that is, Additive White Gaussian Noise (AWGN) and Rayleigh multipath fading channels. The results obtained showed that the performance of the OFDM system is better over the AWGN channel than Rayleigh fading channel for all the modulation schemes. The findings generally revealed that the lower the order of M-ray modulation schemes, the better the BER performance at any given SNR. The BER for both QPSK and 16-QAM improves in the MIMO-OFDM system over the Rayleigh fading channel.

Table 2.1 summarizes literature review findings, method and simulator that was used.

Table 2.1: Summary of literature review

Ref.	**Method**	**Simulator**	**Metric**
[1]	CMPVoD	OMNeT++	Packet loss, throughput
[2]	packet-level encoding technique	ns-3	Latency PSNR
[4]	ZAG+	ns-2	PSNR
[7]	handover algorithms	ns-3	Packet loss, throughput Latency
[8]	TCP-FSO	Matlab	Packet lost, throughput

[11]	congestion control algorithms	ns-3	Packet loss, throughput Latency

Chapter 3

SIMULATION MODEL ARCHITECTURE

The simulation was carried out by converting a video to a digital signal and sending it over an end-to-end 5G physical layer in the MATLAB 2020a environment. The physical layer is liable for coding as well as hybrid-ARQ processing, modulation, multi-antenna handling, and mapping of a signal to the correct physical time-frequency resources (Figures 3.1 and 3.2). The 5G LTE mobile communication infrastructure uses the same access stratum as the 4G LTE, which handles the mapping of transport channels to physical channels. Therefore, the data is grouped in a very rational manner to allow for distribution over the 5G New Radio (NR) radio access network. There are several different modifications done for the data to be communicated over the radio communication channel. First, they need to be clearly labeled and have specified positions and formats [31, 32, 33]. Secondly, The data needs to be labeled and should have specified positions and formats in order for it to be communicated over the radio communication channel.

3.1 5G Downlink and uplink channel mapping

The terminology for the uplink and downlink networks is the same as for 4G LTE. For the downlink, the names of the channels and the information used for the 5G communication system are described below [33].

The links between the user facility and the base station also require many networks mapped to the same degree as the downlink to the 5G mobile communications infrastructure.

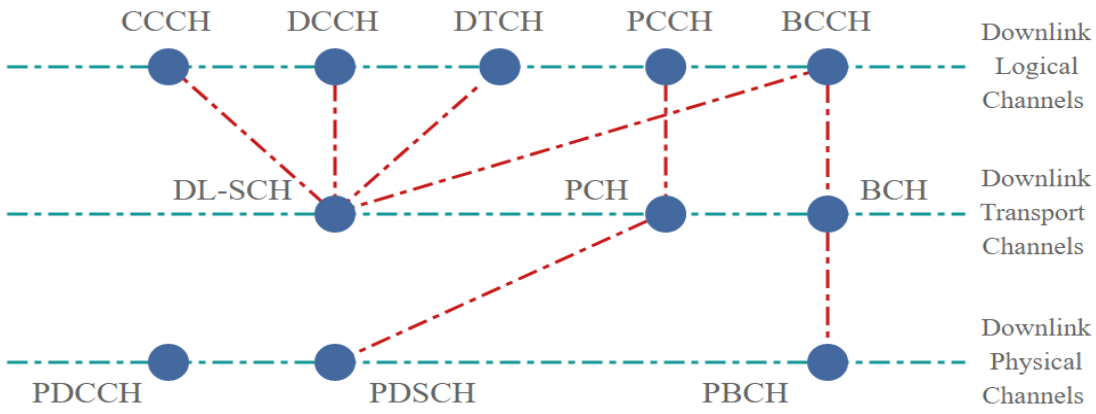

Figure 3.1: 5G NR Downlink Share channel mapping [13]

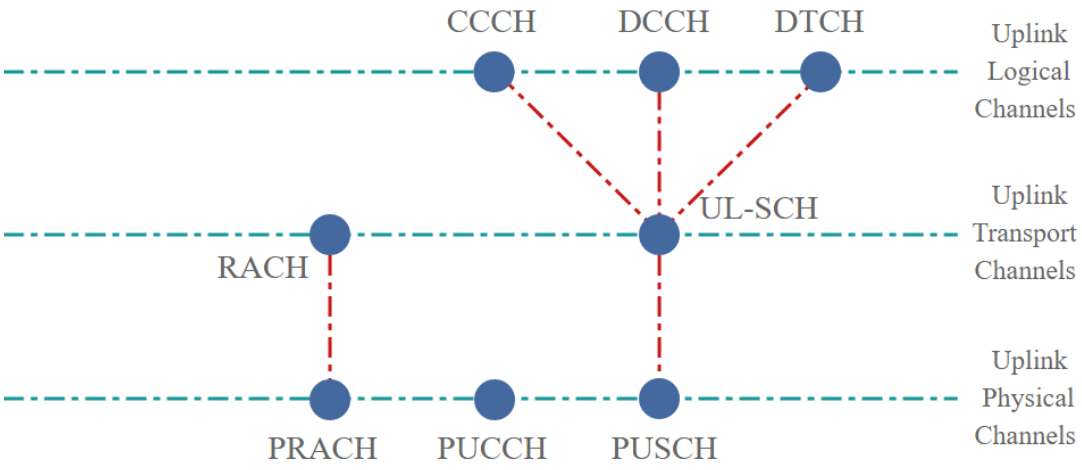

Figure 3.2: 5G NR uplink Share channel mapping [12]

The abbreviations are listed below in accordance to type of channels:

Logical Channel

Broadcast Control Channel BCCH

Paging Control Channel PCCH

Common Control Channel CCCH

Dedicated Control Channel	DCCH
Multicast Control Channel	MCCH
Dedicated Traffic Channel	DTCH
Multicast Traffic Channel	MTCH

Transport Channel

Broadcast Channel	BCH
Downlink Shared Channel	DL-SCH
Paging Channel	PCH
Multicast Channel	MCH
Uplink Shared Channel	UL-SCH
Random Access Channel	RACH

Physical Data Channel

Physical downlink shared channel	PDSCH
Physical broadcast channel	PBCH
Physical multicast channel	PMCH
Physical uplink shared channel	PUSCH
Physical random-access channel	PRACH

Physical Control Channel

Physical control format indicator channel	PCFICH
Physical Hybrid ARQ indicator channel	PHICH
Physical downlink control channel	PDCCH
Relay physical downlink control channel	R-PDCCH
Physical uplink control channel	PUCCH

In mobile communication networks, these three major types of data channels can be referred to as 5G networks, and the hierarchy is shown below respectively.

- Logical channel: Provide services to the Medium Access Control (MAC) layer within the LTE protocol system. Logical channels could be one of two different groups: control channels or traffic channels:
    - Control channels: Control channels are used to transfer data from the control plane.
    - Traffic channels: The logical traffic channels are used for the flow of data from the user aircraft.
- Transport channel: Physical layer transport channels provide information flow to MAC (Medium Access Control) and higher layers.
- Physical channel: they are channels of transmission that carry the user data. Controlled messages are nearest to the direct transmitting of data over the 5G radio frequency (RF) radio access network. They are used to relay data over the radio interface.

  Physical channels often have relatively high channels mapped to provide a specialized service. For example, physical channels hold payload data or information on specific data transmission characteristics such as modulation, reference signal multiplexing, transmitting power, and RF power.

3.2 System model

The system model of video streaming over mmWave is performed with system-level simulation using the downlink physical layer, which is seen as a combination of the transport channel (DL-SCH) and the Physical Downlink Shared Channel (PDSCH),

(Figure 3.3). The end-to-end baseband signal processing procedures are discussed in the following sections, in which we consider input and output as the sample video.

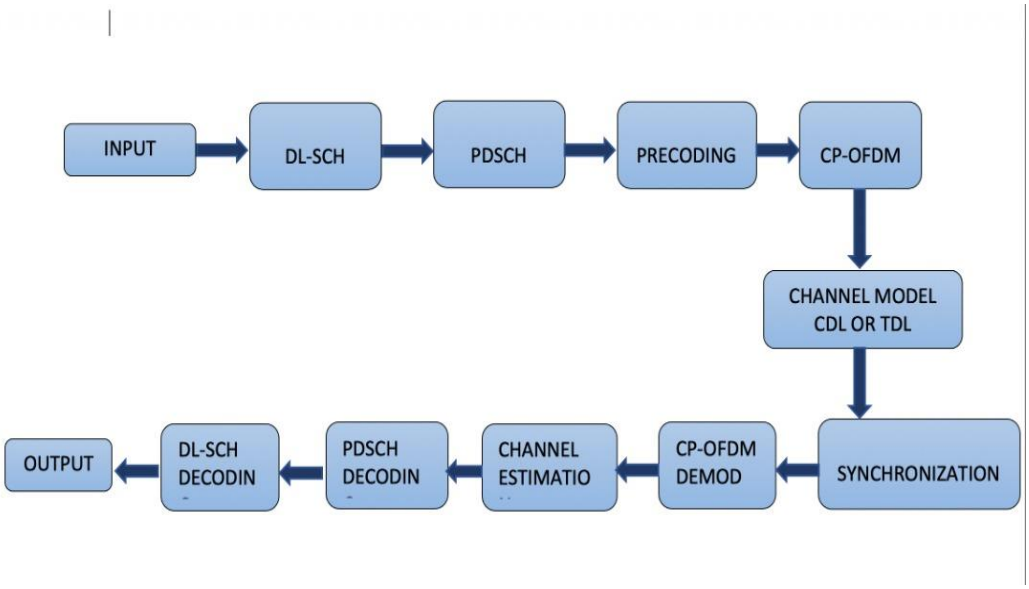

Figure 3.3: End-to-end simulation structure of 5G [34]

3.2.1 Input

A video compression process was performed at the input, converting digital video into a format that takes up less capacity when stored or transmitted to produce a compressed bitstream. Video compression (or video coding) is an essential technology for digital television, DVD-Video, mobile TV, videoconferencing and internet video streaming.

3.2.2 The Downlink Shared Channel (DL-SCH)

It is the principal transportation medium used for downlink data transmission in 5G NR. It is the main transport channel used for transmitting downlink data, and it supports all the key 5G NR features. These include dynamic rate adaptation, HARQ, channel-aware scheduling, and spatial multiplexing. The DL-SCH is also used to transmit certain parts of the BCCH system information, specifically the System Information Block (SIB). Each UE has a DL-SCH for each cell to which it is connected [34].

3.2.3 Physical Downlink Shared Channel (PDSCH)

The PDSCH is the main data-bearing channel assigned to users on a complex and opportunistic basis. The PDSCH holds the data in what is known as Transport Blocks (TB), which correspond to the MAC PDU. They are transferred from the MAC layer to the PHY layer once per Transmission Time Interval (TTI) (i.e. 1ms scheduling interval) to meet low latency requirements. A convolutional turbo coder is used for forwarding error correction in order to avoid channel propagation errors. The data is mapped to spatial layers according to the type of multi-antenna technique (e.g. closed-loop, open loop, spatial multiplexing, and transmission diversity) and mapped to a modulation symbol that contains 16 Quadrature Amplitude Modulation (QAM) and 64 QAM. Physical resources are allocated to one TTI based on two resource blocks (1ms). It is referred to as the 'pair of resource blocks' and is the sum of resources that can be distributed. This corresponds to 12 sub-carriers (180 kHz) for 14 OFDM symbols (normal cyclic prefix (CP) mode) [35].

3.2.4 Precoding

mmWave signals experience a more pathless order of magnitude than the microwave signals presently used in most wireless applications and cellular systems. mmWave systems must also exploit large antenna arrays to combat path loss with a beamforming gain by reducing wavelength. Multiple data stream forming, known as precoding, is used to further focus on strengthening the spectral efficiency of mmWave. Both beamforming and precoding were performed on a digital basis in conventional multi-antenna systems. However, the higher cost and power usage of mixed-signal equipment in mmWave systems make analog processing in the RF domain more attractive [35].

3.2.5 Orthogonal frequency-division multiplexing (OFDM)

Single-User MIMO-OFDM system for which a maximum number of transmission and receiving antenna components could be 1024 and 32, with up to 16 independent data streams. Models are a spatial channel where array positions and antenna patterns are integrated into the overall system architecture. OFDM has become an extensively implemented numerical modulation method for wireless communication, such as Wireless Local Area Network (WLAN), LTE, Digital Video Broadcasting-Terrestrial (DVB-T), and 5G. OFDM is part of the multi-carrier modulation group. OFDM divides into smaller neighboring (carriers) sub-bands around the transmitted frequency band, and each carrier is modulated separately. With the Inverse Fast Fourier Transformation (IFFT), this modulation approach can be extended. The OFDM signal gains power over the frequency-selective fading channel, eliminates neighboring sub-carrier's crosstalk, and uses small orthogonal subcarriers [36,37].

The OFDM signal collects data into a time-domain waveform distributed across the air using orthogonal single-carrier frequency-domain waveforms. As its primary modulation type, subscribers use QPSK or QAM.

The equation of inverse discrete Fourier transforms is:

$$f(x) = \frac{1}{N}\sum_{t=0}^{N-1} F(x)e^{i\frac{2\pi xt}{N}}$$

Different OFDM-based systems have been discussed during the 5G specification. It is used in LTE and chosen as a 3GPP Significance 15 standard by OFDM cyclic prefix (CP-OFDM). At the beginning of the OFDM symbol, the whole process adds a high-level signal called a cyclic prefix. CP-OFDM promotes inter-symbol interference (ISI) and inter-carrier interference (ICI) by data entry for a certain period, i.e., from the

trailed end of the OFDM symbol as a cyclic prefix to the beginning of the OFDM symbol. This symbol represents the signal constellation for the MQAM subcarrier, i.e., 16-QAM, 64-QAM, and so on.

3.2.6 Channel model

The channel model is a statistical representation of the results of a transmission channel by which wireless signals are transmitted. For example, the channel model may reflect the power loss caused by the signal as it passes through the wireless medium. In a more general case, the channel model is the impulse response of the channel medium in the time domain or its Fourier transformation in the frequency domain. Usually, the channel impulse response of a wireless communication device varies randomly over time. Using channel models with wireless system design in MATLAB and Simulink has provided optimize system reliability, performs system architecture tradeoffs, and provides a realistic assessment of overall system performance.

We considered Tapped Delay Line (TDL) channel model in a downlink MIMO system with 1 Base Station (BS) equipped with four transmitter antennas and 1 Mobile Station (MS) also equipped with four receiver antennas. The channel impulse response of the TDL channel model can be defined as [38]:

$$H(t,\tau) = \sum_{i=1}^{n} a_i(t)\delta(\tau - \tau_i)$$

where $a_i(t)$ refers to the amplitude at the τ_i delay for the ith tap.

3.2.7 OFDM Demodulation

An OFDM demodulator demultiplexes a multi-subcarrier time-domain signal using an OFDM modulation. The OFDM demodulation uses an FFT operation that results

in *N* parallel data streams. It consists of a bank of *N* correlators, with one correlator assigned to each OFDM subcarrier, followed by a parallel-to-serial conversion [39].

3.2.8 Channel Estimation

Channel estimation plays an essential part in an OFDM system. It is used for increasing the capacity of orthogonal frequency division multiple access (OFDMA) systems by improving the system performance in terms of bit error rate.

LTE uses cell-specific reference signals (pilot symbols) inserted in both time and frequency to estimate the channel characteristics. These pilot symbols provide an estimate of the channel at given locations within a subframe. Through interpolation, it is possible to estimate the channel across an arbitrary number of subframes.

The use of equalization and channel estimation is necessary for OFDM to improve its BER performance against the impairments of the multipath fading channel. Pilot insertion in the OFDM system can be two-dimensional (2-D) or one-dimensional (1-D). 2-D pilot insertion techniques outperform 1-D pilot insertion techniques; however, the high complexity associated with 2-D pilot insertion techniques have made them unattractive for use in practical systems [40].

3.2.9 PDSCH Demodulation

Decoding is the inverse of Physical Downlink Shared Channel (PDSCH) processing on the matrix of complex modulated PDSCH symbols. It depends on the cell-wide settings structure and channel-specific configuration structure of PDSCH. The channel inverse processing includes the decoding, layer demapping and codeword separation, soft demodulation and descrambling. The decoding is performed using matrix pseudo inversion of the precoding matrices. For applications involving propagation channels

or noise, channel estimation and equalization are done on the received symbols before decoding [41].

3.2.10 DL-SCH Demodulation

The Downlink Shared Channel (DL-SCH) decoding includes rate recovery, turbo decoding, block concatenation and CRC calculations. Alternatively, the function lteDLSCHDecode [39] also provides the same functionality. In addition, this function also retains the type-24B code block set CRC decoding result, the HARQ process decoding state and provides parameterization for specifying the initial HARQ process state [42].

3.2.11 Output

The compressed bitstream is decoded, with each of the syntax elements, and the extracted information is described as quantized transform coefficients, prediction information, etc. This information is then used to reverse the coding process and recreate a sequence of video images [43].

Chapter 4

SIMULATION SETUP, RESULTS AND DISCUSSION

4.1 Simulation Setup and Performance Metrics

MATLAB is supported with a 5G library in the LTE Framework Toolbox. It enables simulation of the critical characteristics of a 5G network system, including 5G NR physical channels and signal generation. The 5G library is defined for version 15 of the 5G NR specification [7,29]. The steps of the simulation are as follows:

step 1.. A MATLAB function was used to read the video frames as a stream of bytes, which was then converted to bitstream and then transmitted in the form of a bitstream.

step 2.. The video bitstream was transmitted into the downlink shared channel (DL-SCH) and then modulated and mapped into the physical downlink shared channel (PDSCH).

step 3.. The generated data were modulated and coded according to the related modulation coding schemes (MCS).

step 4.. OFDM modulation was applied with the use of the coded data.

step 5.. Additive White Gaussian Noise was applied to the data to strive for a noisy channel. Finally, synchronization and OFDM demodulation were performed using the data.

step 6.. Then data was demodulated and decoded by using the result of channel estimation.

step 7.. Following cyclic redundancy check results, if data was successfully received, then the new data was generated (move back to step 1); otherwise, the data was retransmitted.

BER Computation

Analytical BER calculation was performed by the following equations from [26]. In the formulas, the tail probability of the standard normal distribution dependsed on the modulation scheme as defined by IEEE 802.11 standard.

4QAM $BER_{.}^{14QAM}(\gamma_s) = \frac{1}{2}Q\left(\sqrt{\gamma_s}\right)$

16QAM $BER_{.}^{16QAM}(\gamma_s) = \frac{3}{2}Q\left(\sqrt{\frac{1}{5}\gamma_s}\right)$

64QAM $BER_{.}^{16QAM}(\gamma_s) = \frac{7}{12}Q\left(\sqrt{\frac{1}{21}\gamma_s}\right)$

where γ_s is the SNR value, depending on the type of modulation scheme use (4QAM, 16QAM, 64QAM).

In the simulation, BER computation was performed using the "biterr" function. The "biterr" function compares two sets (input and output) of data and computes the number of BER. An error is a difference between corresponding points in the two sets of data. The two sets of data typically represent messages entering a transmitter and recovered messages leaving a receiver.

Throughput Computation

Analytical computation of the throughput was performed in terms of the number of successfully transmitted packets per time. Since throughput depends only on a channel,

we conveniently used BER to determine the correct bits' throughput. We used the following formula to calculate the throughput (TH) as

$$TH = R * (1 - BER) \log_2(M)$$

where R = source bit rate = 1 , M = no of QAM (4, 16, 64).

The simulation of throughput computation uses 5G Toolbox functions to generate a multi-antenna downlink Reference Measurement Channel (RMC) R.12. Transmission was simulated using the Extended Pedestrian A (EPA) propagation channel model. Channel noise was added to the received waveform, which was then OFDM demodulated, resulting in a received resource grid for each receive antenna. Channel estimation was performed to determine the channel between each transmit/receive antenna pair. The PDSCH data was then extracted and decoded from the received resource grid. Using the result of the block CRC, the throughput performance of the transmit/receive chain was determined.

End-to-end Delay Computation

End-to-end is also referred to as analog-to-analog or mouth-to-air delay. It is the time taken for a packet to pass from one node (UE) to another (UE). This delay includes network delay, encoding delay, decoding delay and compression and decompression delay. The VoIP application can only experience the delay of the sender, the delay of the network, and the receiver's delay, while the video conferencing may experience all the delays mentioned. We computed analytical delay as,

End-to-end delay = ∑(arrive time – send time) / ∑ Number of connections.

To find delay, we used the "xcorr" function of the simulation to determine the cross-correlation between each pair of signals at all possible lags specified by the user. The

normalized cross-correlation between each pair of signals was then calculated. Finally, the estimated delay was given by the negative of the lag for which the normalized cross-correlation has the largest absolute value.

4.2 Results of Simulation

In our calculation of the performance metrics results, we analyzed the analytical and simulation results based on different scenarios (using varied parameters) and consider existing research results to compare our results. The simulated results were based on the system function and analytical results were based on the formula and theories to validate the simulated work by varying the SNR, mmWave carrier frequency, and mmWave bandwidth. We presented graphs of each scenario with the use of given parameters in Table 4.1.

Table 4.1: Table of simulation parameters

Parameter	**Value**
Number of frames	141frames
Frame size	2457600 bits
Duration of video	4.7 s
Frame rate	30 fps
mmWave Bandwidth	1 GHz (varied)
mmWave carrier frequency	28 GHz (varied)
LTE carrier frequency (DL)	2.1 GHz
LTE carrier frequency (UL)	1.9 GHz
LTE bandwidth	20 MHz
Channel SNR	20 dB (varied)

4.2.1 Impact of Scheduling Different QAM Modulation on Throughput and BER by varying the SNR

We compared the throughput and the BER performances of different QAM modulation schemes at different SNR values.

Typical variations in throughput performance with varying SNR values (from -15 dB to 35 dB) for QAM scheduling schemes are presented in Figure 4.1 under a constant: mmWave carrier frequency= 28 GHz, QAM (M = 4, 16, 64), mmWave bandwidth =1 GHz. We observed that at low SNR values, from −15 to -5 dB, the simulated and analytical results demonstrated a low-performance in throughput while QAM 64 modulation scheme presented maximum throughput performance as 4.6 Mbps and 14 Mbps in analytical and simulated results respectively at 35 dB. We also observed a drastic increase in throughput as the SNR increases in both the simulated and analytical results.

As observed from the existing results in [7], as the SNR increases, the throughput also increases and reaches maximum throughput at some SNR values in different modulation schemes. Existing results presented in Figure 4.1 (c) are collected from the physical layer with different parameters and simulator. We considered the characteristics behavior of the throughput to SNR that showed the same trend of our throughput performance results.

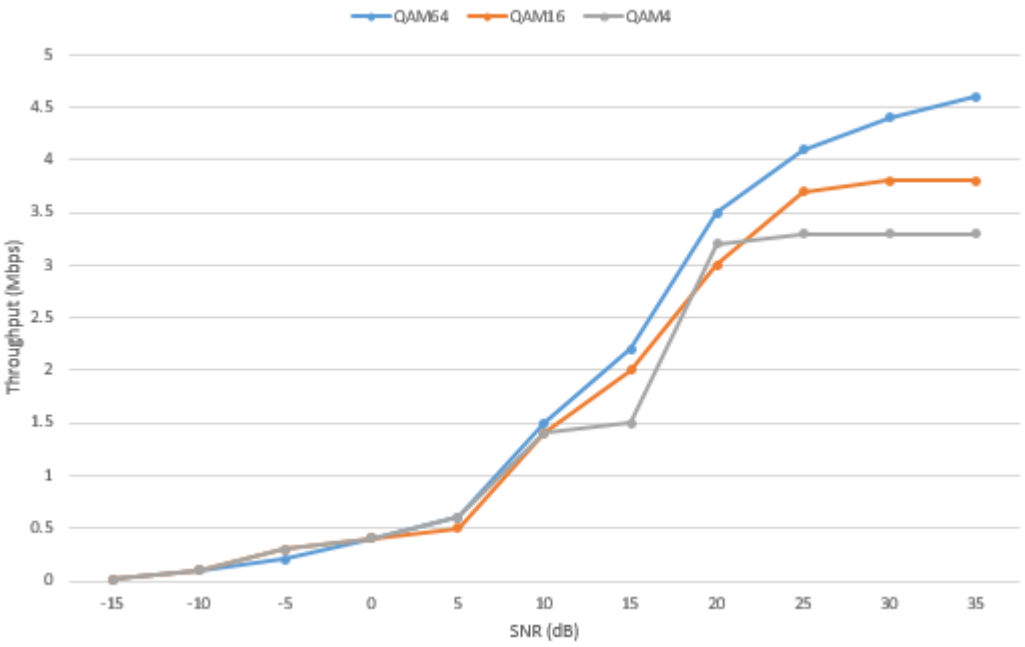

(a) Analytical results

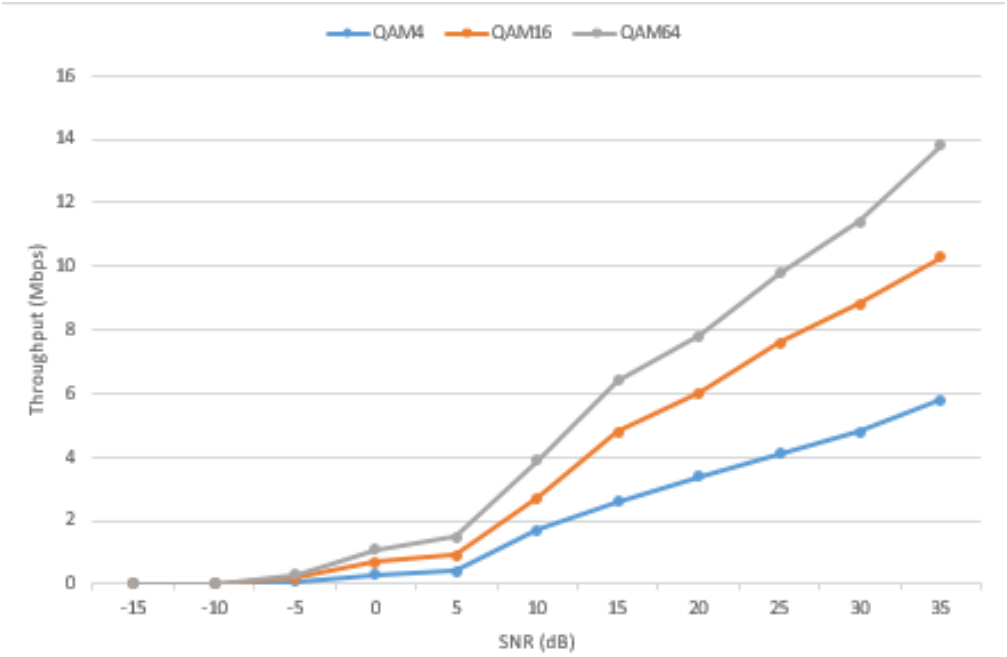

(b) Simulated results

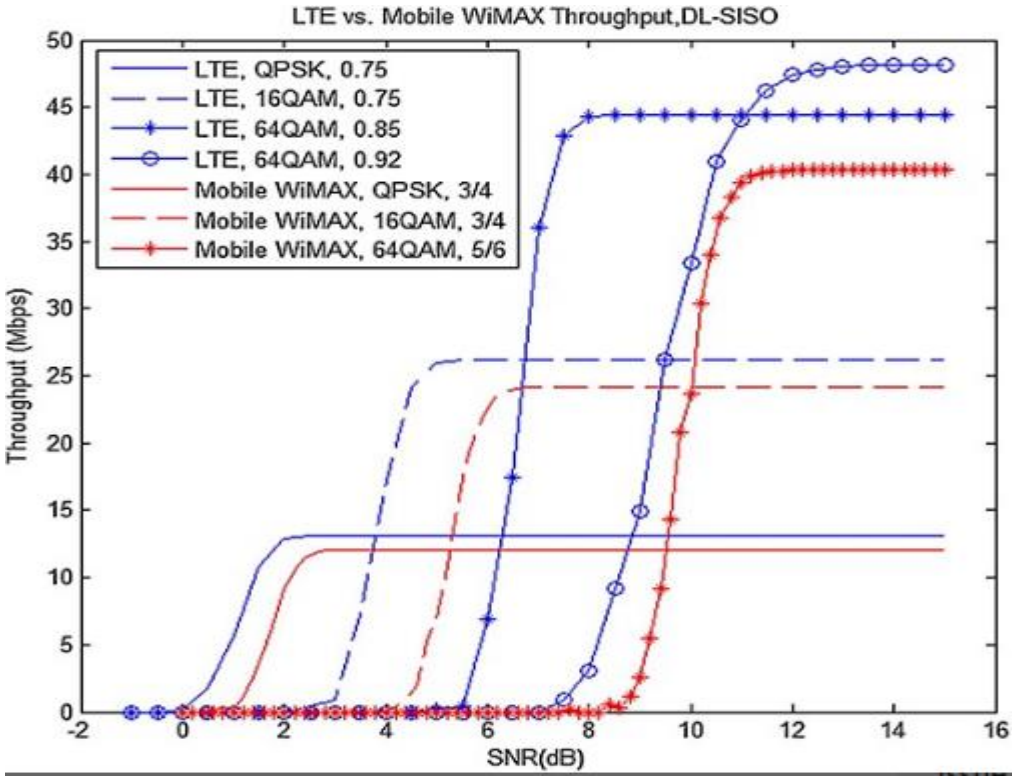

(c) Existing results

Figure 4.1: Throughput vs SNR with mmWave carrier frequency=28 GHz, QAM (M=4,16,64), mmWave bandwidth=1 GHz

Figure 4.2 presents BER versus SNR at different QAM modulation schemes over a mmWave transmission. From the analytical results it is observed that at low SNR ranged from -15 dB to -10 dB in all types of QAM modulation schemes, observed BER is 0.6 which is the highest value. In general while SNR is increasing BER is decreasing in both the simulated and analytical results since signal power is increases in the transmission. When we considered different modulation schemes (M=4, 16, 64) at the same SNR value (e.g. 5 dB) BER increases as M increases in the QAM modulation. The reason for this is that QAM uses the modulation scheme for short-range applications. Some phase noise in this transmission may also be due to imbalance resulting from digital quadrature modulation. It happens before the conversion, and happens at a high level. An increased in M will depend on a larger

value within the same BER. It is therefore good to lower the value using the forward error correction.

When we considered the trend of existing results, as shown in Figure 4.2 (c) from [43], the value of BER decreases as the value of SNR increases in all types of QAM schemes together with M=4, 16, 64, etc.

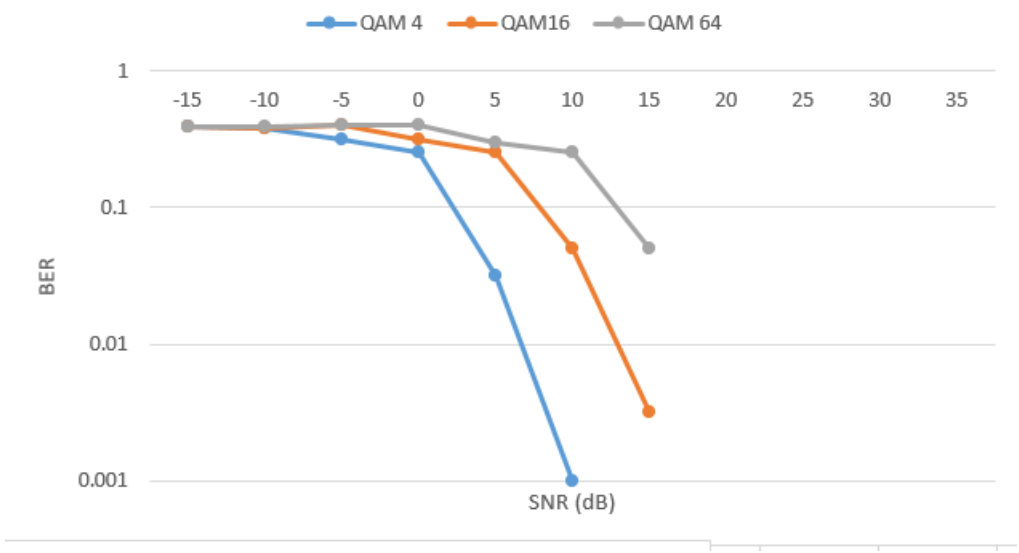

(a) Analytical results

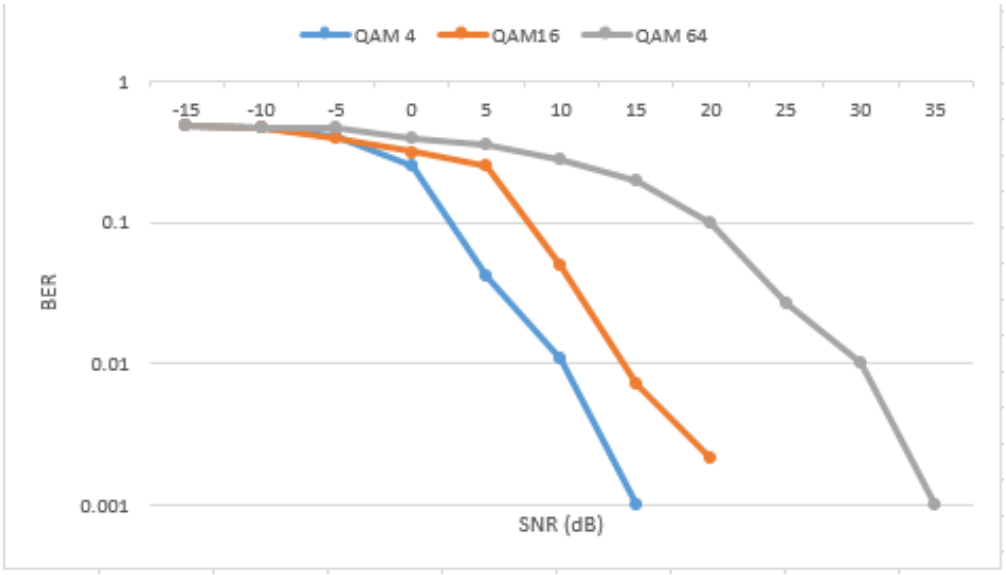

(b) Simulated results

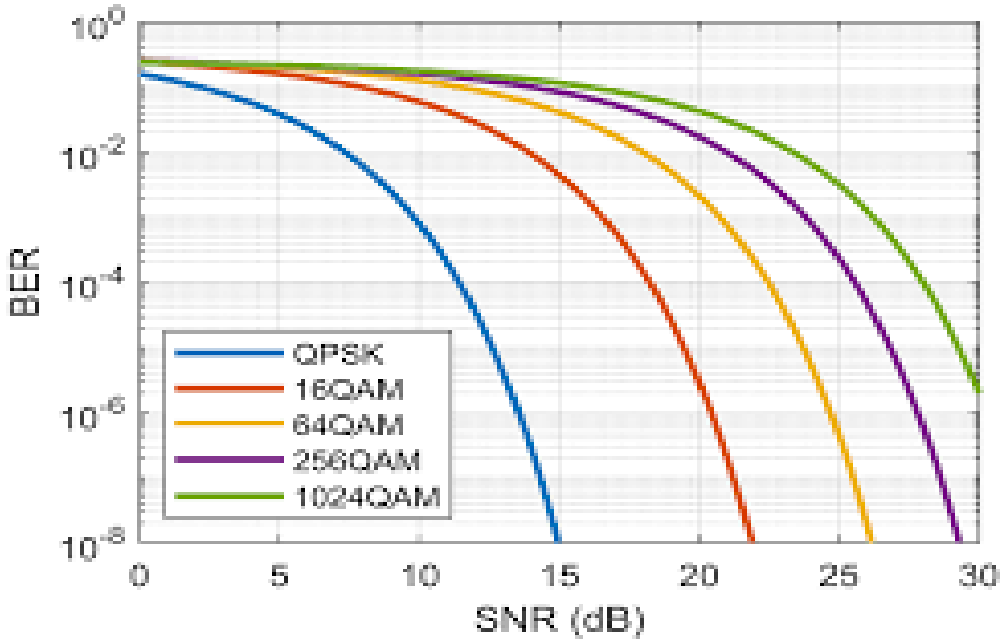

(c) Existing results

Figure 4.2: BER vs SNR with mmWave carrier frequency=28 GHz, QAM (M =4,16,64), mmWave bandwidth=1 GHz

4.2.2 Impact of varying mmWave Carrier Frequency on Throughput and BER

Figure 4.3 illustrates the performance of simulated and analytical calculations on throughput by changing mmWave carrier frequency (28:20:128) at QAM 16 modulation, 20 dB SNR and mmWave bandwidth=1 GHz. The simulated results start with a low throughput of 1Mbps, on the other hand analytical results start with 2 Mbps with mmWave carrier frequency of 28GHz. There is a linear increase as the mmWave carrier frequency increases with a maximum throughput of 6 Mbps and 9 Mbps for the simulated and analytical results, respectively with 128 GHz carrier frequency.

The characteristics behavior of the results shown in Figure: 4.3 (c) from [8], which is base on different parameters and channels on the physical layer, also shows a linear increase in throughput with respect to the carrier frequency.

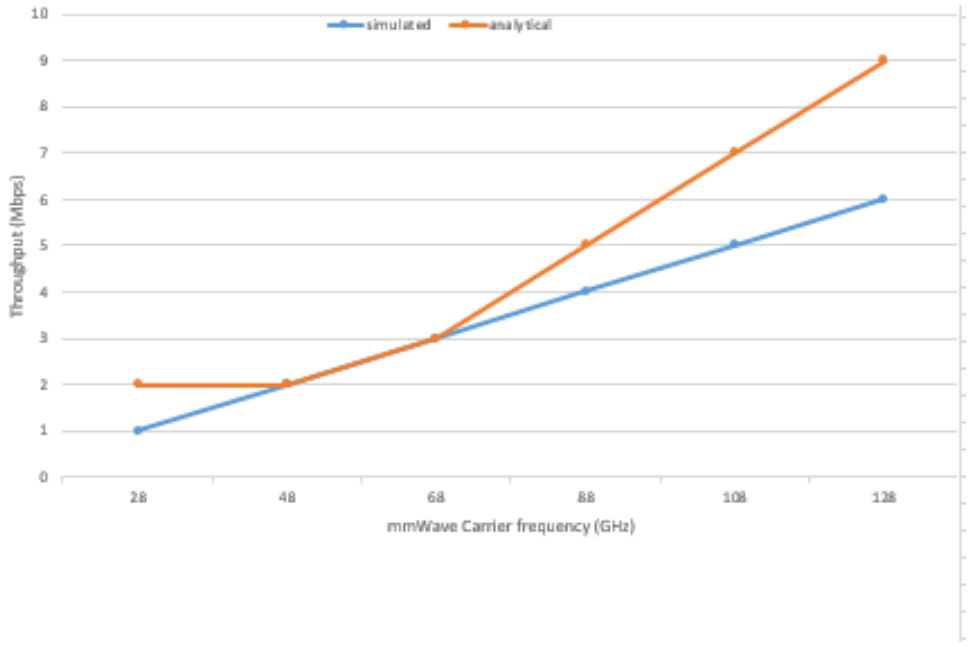

(a) Simulated and analytical results

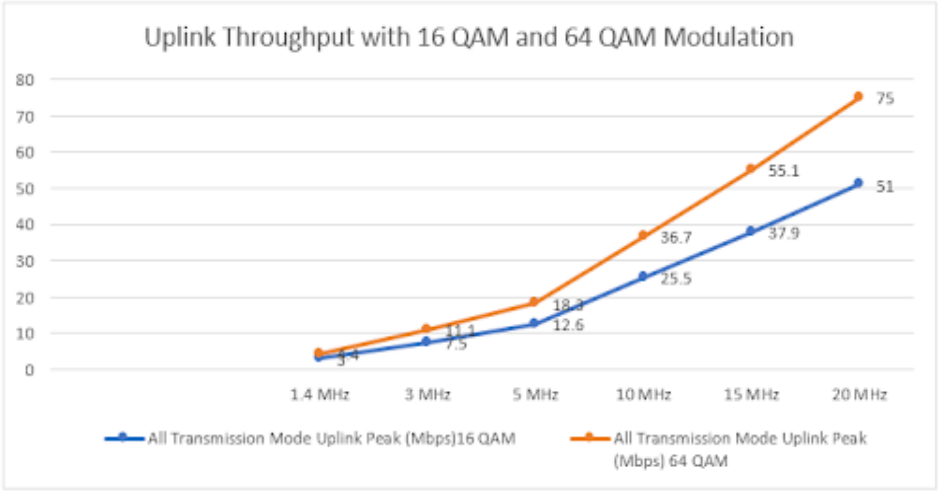

(b) Existing results

Figure 4.3: Throughput vs mmWave carrier frequency with SNR=20 dB, QAM 16, mmWave bandwidth=1 GHz

Figure 4.4 illustrates the performance of BER to varied mmWave carrier frequency at SNR=20 dB, QAM 16 and mmWave bandwidth=1 GHz. The illustration shows that the simulated and analytical results at the lower frequency (28 GHz) starts with a BER of 0.42 and 0.48, respectively. Then, as carrier frequency increases, BER slightly decreases in both simulation and analytical results. The main advantage of higher

frequency is that they require shorter antennas for decent reception quality, which is essential for a mobile device. In addition, it allows a broader band for modulating signals to obtain lower BER in transmission. Figure 4.4 (b) from [34] shows similar characteristic behavior of BER to the carrier frequency, which is based on different parameters and simulation environments.

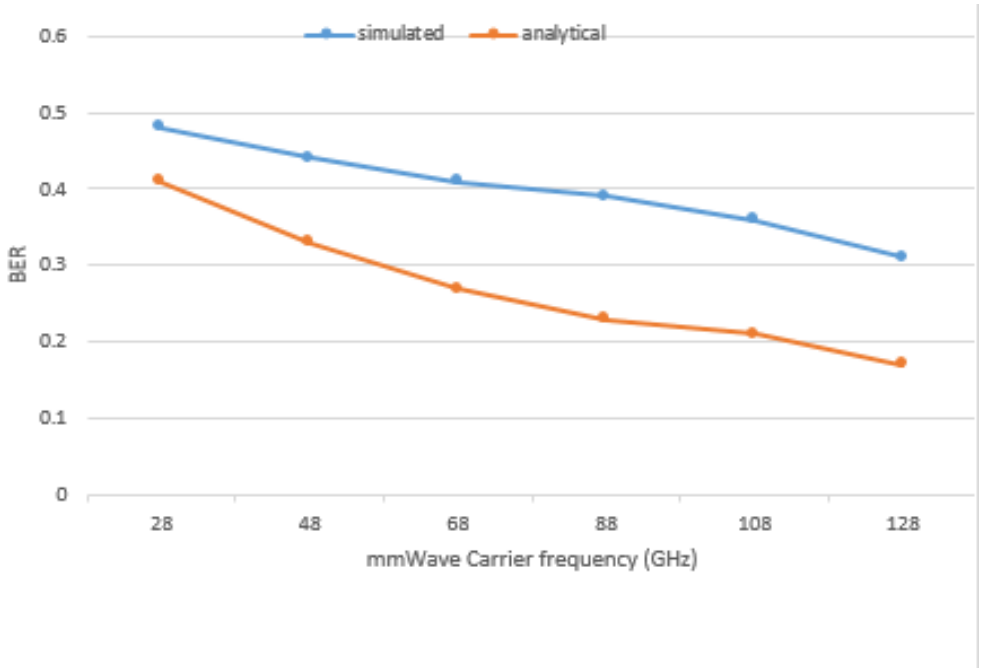

(a) Simulated and analytical results

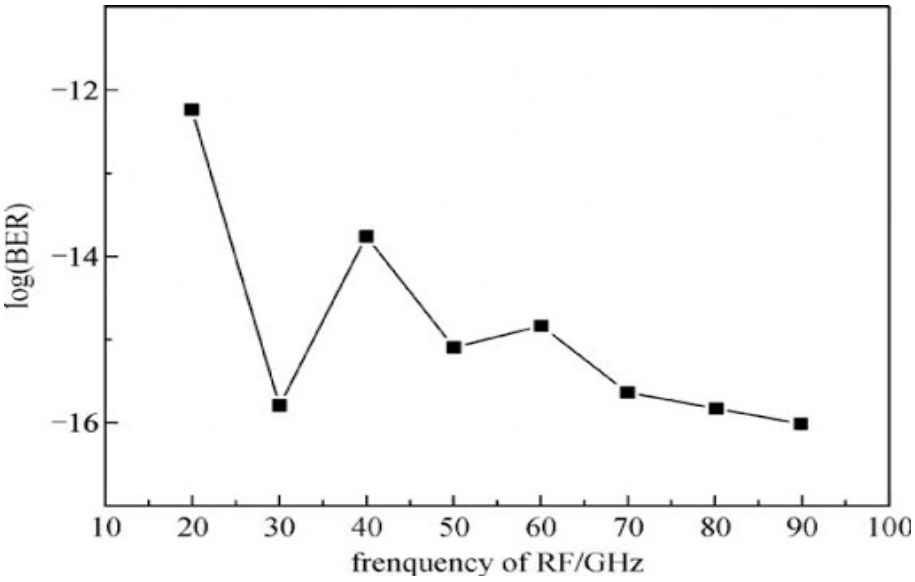

(b) Existing results

Figure 4.4: BER vs. mmWave carrier frequency with SNR=20dB, QAM 16, mmWave bandwidth=1 GHz

4.2.3 Impact of varying Bandwidth on Throughput, BER, and End-to-end Delay

In this section, analytical and simulation performance on throughput, BER, and end-to-end delay against mmWave bandwidth at constant SNR=20dB, mmWave carrier frequency = 28 GHz with QAM 16 was considered.

Figure 4.5 presents BER results to mmWave bandwidth. From both simulation and analytical results, it is observed that, in general, as mmWave bandwidth increases, BER decreases. For example, in Figure 4.5 (a), the simulated result has achieved 0.68 of BER at the lowest bandwidth (0.1GHz). On the other hand, the analytical result has achieved 0.85. Furthermore, the simulated results indicate a decrease in BER as bandwidth increases up to 0.8 GHz. At the same time, the analytical results have a maximum BER of 0.85 at the lowest bandwidth and drastically decrease as the bandwidth increases by 1 GHz. It means if the medium between the transmitter and receiver is suitable and the bandwidth is high, then the bit error rate will be very small

- possibly insignificant and having no noticeable effect on the overall system performance. Figure 4.5 (b) from [35] shows the trend of BER performance to the bandwidth, that is, the BER is relatively high at lower bandwidth and decreases as the bandwidth increases.

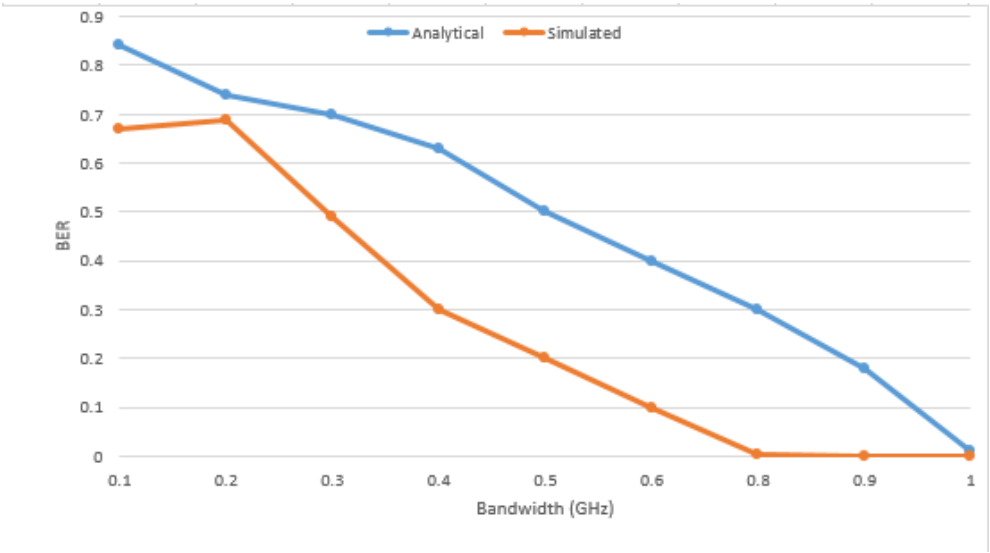

(a) Simulated and analytical results

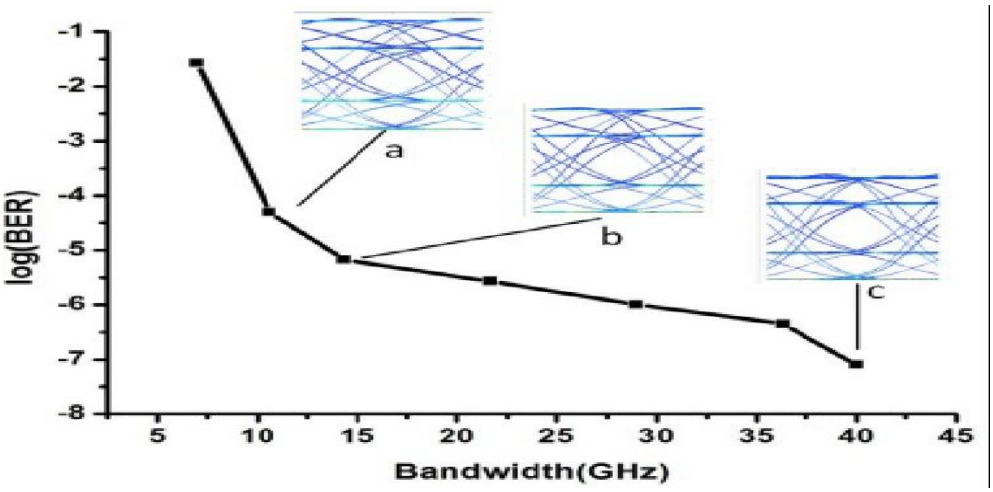

(b) Existing results

Figure 4.5: BER vs mmWave bandwidth with SNR=20dB, mmWave carrier frequency=28 GHz, QAM 16

Figure 4.6 shows simulated and analytical results of throughput to mmWave bandwidth. The results show that at low bandwidth (0.1 GHz), throughput is the lowest, and as bandwidth increases, it increases slowly. Analytical throughput results are better than simulation results in all bandwidths (e.g., at 1 GHz, analytical throughput is 100 Mbps and simulation throughput is 70 Mbps). That means there are some environmental effects in the simulation which affect throughput. Figure 4.4(b) from [10] shows the throughput trend with respect to the bandwidth. That is, the throughput performance linearly increases as the bandwidth increases.

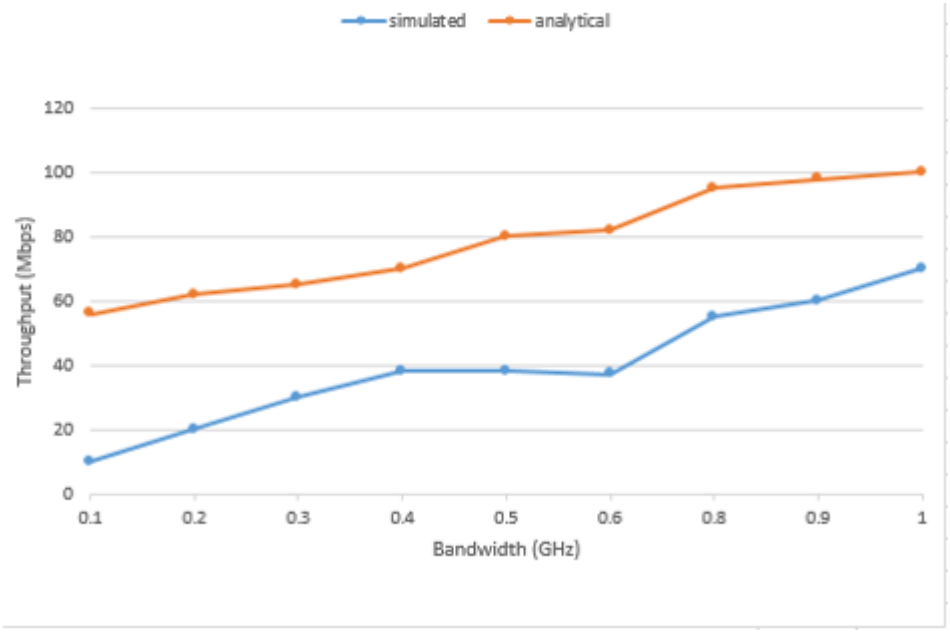

(a) Simulated and analytical results

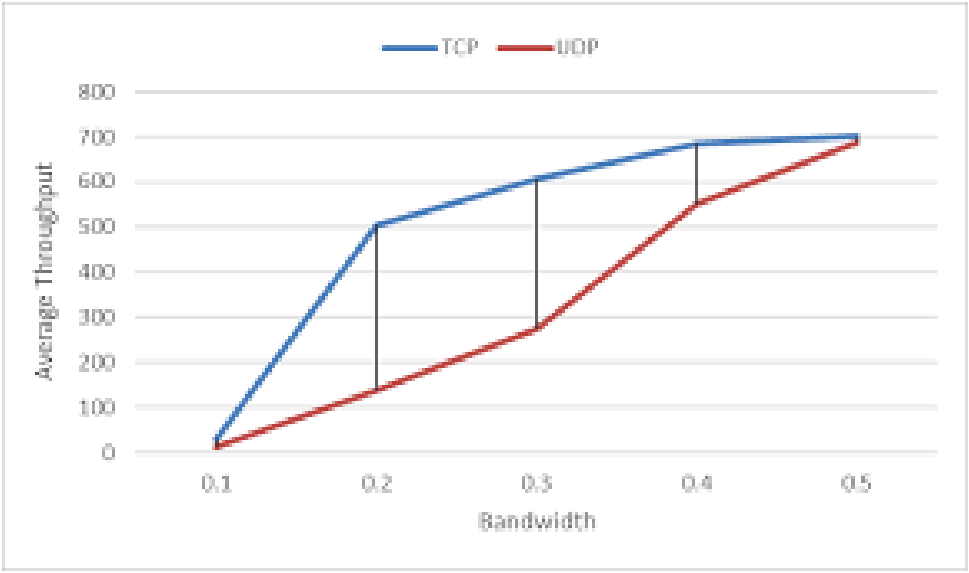

(b) Existing results

Figure 4.6: Throughput vs mmWave bandwidth with mmWave carrier frequency=28 GHz, SNR=20dB, QAM 16

Figure 4.7(a) shows analytical and simulation results of end-to-end delay with respect to mmWave bandwidth. In general, end-to-end delay decreases as bandwidth increases in both cases, whereas analytical results are better than simulation results. End-to-end

delay at the lowest bandwidth (0.1 GHz) has a maximum delay between 3s and 3.7s in the analytical and simulated results. It decreases as the bandwidth continues to increase. Since transmission delay is inversely promotional with data rate, we have a minor delay with large bandwidth.

Figure 4.7(b) from [10] shows the trend of end-to-end delay with respect to bandwidth. As bandwidth increases, delay decreases. Our simulations are based on the physical layer. In our comparisons with the existing studies, we considered trend since we could not find any result which is done under the same conditions and parameters.

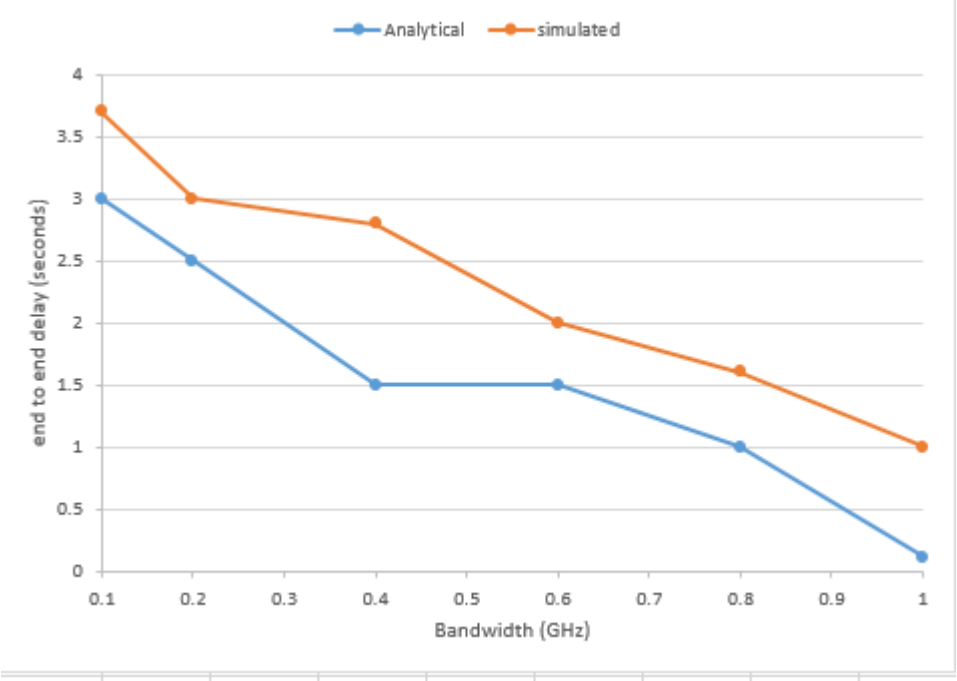

(a) Simulated and analytical results

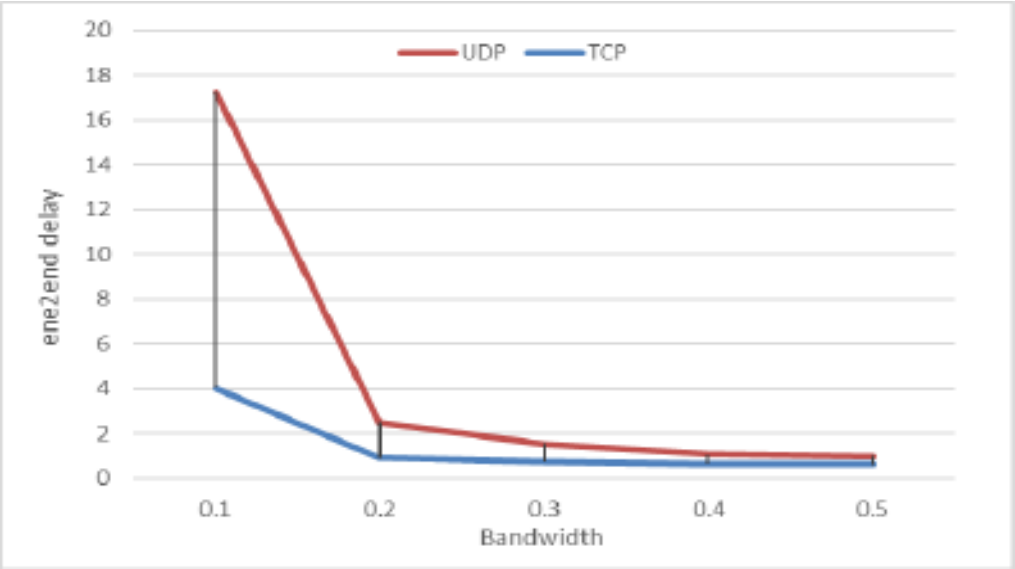

(b) Existing results

Figure 4.7: End-to-end delay vs mmWave bandwidth with mmWave carrier frequency=28 GHz, SNR=20dB, QAM 16,

Theoretically, results show that the reliability of quality video streaming over mmWave connection at high-frequency transmission allows high data rates required to sustain high-quality video source rates. Furthermore, the presented 5G end-to-end video streaming system with a physical layer simulation prevents service inaccessibility during mmWave outages. This makes it easier to enable continuous video streaming at all times.

Chapter 5

CONCLUSION

In this thesis, our interest is investigating video streaming performance over mmWave transmission by evaluating the simulated and analytical results. A high-frequency communication allows the high data rates to sustain the transmission rate at high-quality videos. The challenges were addressed with the end-to-end mmWave channel. The performance was investigated using a 5G toolbox of MATLAB that enables the simulation and calculation of the performance metrics using the downlink physical layer after video compression. The investigation was performed by computing the analytical results and the simulation results for video performance metrics BER, throughput and end-to-end delay throughout the research.

In both simulation and analytical computations of the performance metrics, behaviors were measured by varying QAM schemes, SNR, mmWave carrier frequency and mmWave bandwidth. The results have shown that the characteristic behaviors of the simulated results similar to the analytical results for the parameters evaluated. Therefore, this thesis concluded that the simulated results are reliable compared to the analytical results in terms of all the video performances measured.

Future research is expected to investigate 5G performances of indoor and outdoor with barrier obstacles such as human-body blockage simulation, mobility UE's, and a higher modulation scheme like 256QAM.

REFERENCES

[1] Liu, Fangming & Li, Bo & Zhong, Lili & Li, Baochun & Jin, Hai & Liao, Xiaofei. (2012). Flash Crowd in P2P Live Streaming Systems: Fundamental Characteristics and Design Implications. IEEE Transactions on Parallel and Distributed Systems - TPDS. 23. 1227-1239. 10.1109/TPDS.2011.283.

[2] Drago, Matteo & Azzino, Tommy & Polese, Michele & Stefanović, Čedomir & Zorzi, Michele. (2018). Reliable Video Streaming over mmWave with Multi Connectivity and Network Coding. 508-512. 10.1109/ICCNC.2018.8390387

[3] Pi, Zhouyue, and F. Khan. An introduction to millimeter-wave mobile broadband systems. IEEE Communications Magazine 49.6(2011):101-107.

[4] Rao, Ashwin & Lim, Yeon-sup & Barakat, Chadi & Legout, Arnaud & Towsley, Don & Dabbous, Walid. (2011). Network Characteristics of Video Streaming Traffic. 10.1145/2079296.2079321

[5] Mustafa Ahmed, diaa Elden & Jama, Abdirisaq & Khalifa, Othman. (2015). VIDEO TRANSMISSION OVER WIRELESS NETWORKS REVIEW AND RECENT ADVANCES. International Journal of Computer Applications Technology and Research. 4. 444-448.

[6] M. Bouzian, M. Bouhtou, T. En-Najjary, L. Sassatelli, and G. Urvoy-Keller, "QoE optimization of ON/OFF video streaming strategy in wireless networks," 2016 Wireless Days (WD), Toulouse, 2016, pp. 1-8.

[7] Rezaei, Fahimeh & Hempel, Michael & Sharif, Hamid. (2013). Towards the performance evaluation of 4th generation wireless communication standards: LTE versus Mobile WiMAX. Wireless Communications and Mobile Computing. 15. 10.1002/wcm.2404. M. Okano, Y. Hasegawa, K. Kanai, B.

[8] Wei and J. Katto, "TCP throughput characteristics over 5G millimeterwave network in indoor train station," 2019 IEEE Wireless Communications and Networking Conference (WCNC), Marrakesh, Morocco, 2019, pp. 1-6, doi: 10.1109/WCNC.2019.8886119.

[9] Hou, Yanjun & Zhou, Wen'an & Song, Lijun & Gao, Mengyu. (2017). A QoE Estimation Model for Video Streaming over 5G Millimeter Wave Network. 93-104. 10.1007/978-3-319-49106-6_9.,

[10] F. taha and N.sabi "Performance Comparison between TCP and UDP Protocols in Different Simulation Scenarios" International Journal of Engineering & Technology, 7 (4.36) (2018) 172-176

[11] M. Mezzavilla et al., "End-to-End Simulation of 5G mmWave Networks," in IEEE Communications Surveys & Tutorials, vol. 20, no. 3, pp. 2237-2263, thirdquarter 2018.doi: 10.1109/COMST.2018.2828880.

[12] E. Kohler, M. Handley, and S. Floyd, "RFC4340: Datagram Congestion Control Protocol (DCCP)," *Internet RFCs*, 2006.

[13] Pei D. (2020) Interference Analysis of Mobile Communication Multi-system. In: Huang C., Chan YW., Yen N. (eds) Data Processing Techniques and Applications for Cyber-Physical Systems (DPTA 2019). Advances in Intelligent Systems and Computing, vol 1088. Springer, Singapore. https://doi.org/10.1007/978-981-15-1468-5_85

[14] Mousavi, H., Amiri, I. S., Mostafavi, M. A., & Choon, C. Y. (2019). LTE physical layer: Performance analysis and evaluation. *Applied Computing and Informatics*, *15*(1), 34–44.

[15] V. V. Ryzhakov and E. V. Prokhorova, "Electrocardiogram Signals Digital Processing in a Distributed Computing System," 2020 Systems of Signal Synchronization, Generating and Processing in Telecommunications (SYNCHROINFO), Svetlogorsk, Russia, 2020, pp. 1-5, DOI: 10.1109/SYNCHROINFO49631.2020.9166080.

[16] Mousavi, H., Amiri, I., Mostafavi, M., & Choon, C. (2019). LTE physical layer: Performance analysis and evaluation. Applied Computing And Informatics, 15(1), 34-44. doi: 10.1016/j.aci.2017.09.008.

[17] (PDF) An Adaptive Threshold Feedback Compression Scheme Based on Channel Quality Indicator (CQI) in Long Term Evolution (LTE) System. (2015). *ResearchGate*. https://doi.org/10.1007\/s11277-015-2350-1

[18] R. A. Patil, P. Kavipriya and B. P. Patil, "Bit Error Rate Analysis of 16 X 16 MIMO - OFDM in Downlink transmission for LTE - A," 2018 International Conference on Smart Systems and Inventive Technology (ICSSIT), Tirunelveli, India, 2018, pp. 82-87,

[19] C. B. Barneto, L. Anttila, M. Fleischer and M. Valkama, "OFDM Radar with LTE Waveform: Processing and Performance," 2019 IEEE Radio and Wireless Symposium (RWS), Orlando, FL, USA, 2019, pp. 1-4,

[20] Ok-Sun Park, Dae-Ho Kim and Jae-Min Ahn, "Performance analysis of clustered DFT-Spread OFDM for LTE-Advanced uplink MIMO," 2010 4th International Conference on Signal Processing and Communication Systems, Gold Coast, QLD, 2010, pp. 1-5.

[21] A Comprehensive Review of QAM-OFDM Optical Networks. (2018). ResearchGate. https://doi.org/10.26438\/ijcse\/v6i11.811817

[22] T. Deepa and R. Kumar, (2012). performance of comparison metrics on M-QAM OFDM systems with high power amplifier.World Congress on Information and Communication Technologies, Trivandrum. 909-914.

[23] Tse D, Viswanath P: Fundamentals of Wireless Communications (Cambridge University Press. MA: Cambridge; 2008.

[24] Love DJ, Heath Jr R, Santipach W, Honig M: What is the value of limited feedback for MIMO channels. IEEE Commun. Mag 2004, 42: 54-59. 10.1109/MCOM.2004.1341261

[25] (2020) Video Streaming. In: Tatnall A. (eds) Encyclopedia of Education and Information Technologies. Springer, Cham. https://doi.org/10.1007/978-3-030-10576-1_300708

[26] M.Rashmi, Dr. K. V. Prasad, and K. V. S. C. Sastry, “Generation of 5G Waveforms using MATLAB 5G Toolset,” International Research Journal of Engineering and Technology (IRJET) 2020, vol.2 pp. 1-12

[27] B. Barnett, L. Anttila, M. Fleischer and M. Valkama, "OFDM Radar with LTE Waveform: Processing and Performance," 2019 IEEE Radio and Wireless Symposium (RWS), Orlando, FL, USA, 2019, pp. 1-4,

[28] (2020) Adaptive Video Streaming. In: Shen X.., Lin X., Zhang K. (eds) Encyclopedia of Wireless Networks. Springer, Cham. https://doi.org/10.1007/978-3-319-78262-1_300019

[29] Ok-Sun Park, Dae-Ho Kim and Jae-Min Ahn, "Performance analysis of clustered DFT-Spread OFDM for LTE-Advanced uplink MIMO," 2010 4th International Conference on Signal Processing and Communication Systems, Gold Coast, QLD, 2010, pp. 1-5,

[30] M Elsharief, AH Zekry, M Abouelatta - International Journal of Computer Applications, 2014

[31] Vigilante M., Reynaert P. (2018) Introduction. In: 5G and E-Band Communication Circuits in Deep-Scaled CMOS. Analog Circuits and Signal Processing. Springer, Cham. https://doi.org/10.1007/978-3-319-72646-5_1

[32] T. Deepa and R. Kumar, (2012). performance of comparison metrics on M-QAM OFDM systems with high power amplifier.*World Congress on Information and Communication Technologies*, Trivandrum. 909-914.

[33] Sheshjavani, A. G., & Akbari, B. (2014). A study on repeat-request chunks in pull-based peer-to-peer video-on-demand streaming. 2014 22nd Iranian Conference on Electrical Engineering (ICEE).

[34] Experimental demonstration of non-line-of-sight visible light communication with different reflecting materials using a GaN-based micro-LED and modified IEEE 802.11ac - Scientific Figure on ResearchGate. Available from: https://www.researchgate.net/figure/a-BER-versus-DC-bias-in-VLC-for-50-MHz-optical-carrier-frequency-and-256-QAM-scheme_fig4_328259540.

[35] Chen, Fuping & Shao, Yufeng & Chen, Lao & Shen, Shilu. (2016). 4-Pulsed Amplitude Modulation Optical Downlink Signals Reception in Optical Access Systems Using Different Bandwidth Optical Bessel Filter. Optics and Photonics Journal. 06. 89-93. 10.4236/opj.2016.68B015.

[36] Quality of Service (QoS) for Wireless Video Streaming. In: Shen X.., Lin X., Zhang K. (eds) Encyclopedia of Wireless Networks. Springer, Cham. https://doi.org/10.1007/978-3-319-78262-1_300535

[37] Abdollah Ghaffari Sheshjavani, & Behzad Akbari. (2016, March 11). An adaptive buffer-map exchange mechanism for pull-based peer-to-peer video-on-demand streaming systems. Retrieved February 26, 2020,

[38] Cho, Seongho & Cho, Joonho & Shin, Sung-Jae. (2010). Playback Latency Reduction for Internet Live Video Services in CDN-P2P Hybrid Architecture. IEEE International Conference on Communications. 1-5. 10.1109/ICC.2010.5502573.

[39] Polese, M. (2016). Performance Comparison of Dual Connectivity and Hard Handover for LTE-5G Tight Integration in mmWave Cellular Networks. arXiv.org.

[40] Drago, Matteo & Azzino, Tommy & Polese, Michele & Stefanović, Čedomir & Zorzi, Michele. (2018). Reliable Video Streaming over mmWave with Multi Connectivity and Network Coding. 508-512.

[41] PUSCH Throughput Conformance Test. (2021). Mathworks.com. https://www.mathworks.com/help/lte/ug/pusch-throughput-conformance-test.html

[42] M. E. Hassan, A. E. Falou and C. Langlais, "Performance assessment of linear precoding for multi-user massive MIMO systems on a realistic 5G mmWave channel," 2018 IEEE Middle East and North Africa Communications Conference (MENACOMM), Jounieh, 2018, pp. 1-5,

[43] G. Barb and M. Otesteanu, "On the Influence of Delay Spread in TDL and CDL Channel Models for Downlink 5G MIMO Systems," 2019 IEEE 10th Annual Ubiquitous Computing, Electronics & Mobile Communication Conference (UEMCON), New York City, NY, USA, 2019, pp. 0958-0962, doi: 10.1109/UEMCON47517.2019.8992982.

[44] R. Trifan and A. Enescu, "MU-MIMO Precoding Performance Conditioned by Inter-user Angular Separation," 2018 International Symposium on Electronics and Telecommunications (ISETC), Timisoara, 2018, pp. 1-4, DOI: 10.1109/ISETC.2018.8583919.

APPENDICES

Appendix A: Code for Throughput to SNR

```
%%%%%%%%%%%%%%%%%%%%code %%%%%%%%%%%%%%

clear all

close all

Throughput=[];

v = VideoReader('xylophone.mp4'); % load a video%

D = v.Duration;                  % duration of a video%

framerate=v.FrameRate;           %Number of frames per second

no=v.NumberOfFrames;              % Number of frames%

figure();

for i=1:1:no

frames=read(v,i);                %read all frames in the video

%a=imshow(frames)

b=rgb2gray(frames);              %convert coloured frame to gray scale

% c=imshow(b)                    %show then frame

end

m = reshape(dec2bin(typecast(b(:),'uint8'),8).',1,[])'; %bitstream%

%convert number of bits into a stream%

MyStr=m';

N = 1 ; % the size of each block

maxN = numel(MyStr);

ix0 = 1:N:maxN;

fh = @(X) MyStr(X:min((X+N-1),maxN));

B = arrayfun(fh,ix0,'un',0);

% now B{K} holds the K-th block of N bits of S
```

```
%convert string to double%
matrix = str2double(B); %%%%%%%%%%%% aka m
SNRdB=-15:5:35;                          %Signal to Noise Ratio in dB
SNR=10.^(SNRdB/10);
for k=1:length(SNR)
   x=(2*matrix)-1;
   y=(sqrt(SNR(k))*x)+randn(1,length(matrix));
   BER_Simulated(k)=length(find((y.*x)<0));
   Source_bitrate=1;
   Throughput(k) = (length(matrix)-BER_Simulated(k))*Source_bitrate;
   %Total number of bits in error
end
Throughput=Throughput/length(matrix);
figure()
plot(SNRdB,Throughput,'b-*', 'linewidth' ,2.0);
xlabel('SNR _ db');
ylabel('Through put');
title ('Throughput to SNR');
grid on;
```

Appendix B: Code for Throughput to the mmWave Carrier Frequency

```
clear all;
close all;clc
M = 16; % Modulation order (alphabet size or number of points in signal constellation)
k = log2(M); % Number of bits per symbol
v = VideoReader('xylophone.mp4'); % load a video%
D = v.Duration;                   % duration of a video%
framerate=v.FrameRate;


frames=read(v,1);                 %read all frames in the video
%a=imshow(frames)
b=rgb2gray(frames);
m = reshape(dec2bin(typecast(b(:),'uint8'),8).',1,[])'; %bitstream%
MyStr=m;
N = 1 ; % the size of each block
maxN = numel(MyStr);
ix0 = 1:N:maxN;
fh = @(X) MyStr(X:min((X+N-1),maxN));
B = arrayfun(fh,ix0,'un',0);
% now B{K} holds the K-th block of N bits of S
%convert string to double%
dataIn = str2double(B)'; %%%%%%%%%%%%% aka m
```

```
sps = 1; % Number of samples per symbol (oversampling factor)

% dataIn = randi([0 1],n,1); % Generate vector of binary data
dataInMatrix = reshape(dataIn,length(dataIn)/k,k);
dataSymbolsIn = bi2de(dataInMatrix);
dataMod = qammod(dataSymbolsIn,M,'bin'); % Binary coding with phase offset of
zero
fs = 300;
Carrier_frequency=28:20:128;
BER=[];
for i=1:6
   fc=Carrier_frequency(i);
   y = modulate(dataMod ,fc,fs,'amssb');
   x = demod(y,fc,fs,'amssb');
   SNRdB=20;                              %Signal to Noise Ratio in dB
   snr=10.^(SNRdB/10);
   receivedSignal = awgn(x,snr,'measured');
   dataSymbolsOut = qamdemod(receivedSignal,M,'bin');
   dataOutMatrix = de2bi(dataSymbolsOut,k);
   dataOut = dataOutMatrix(:); % Return data in column vector
   [numErrors,ber] = biterr(dataIn,dataOut);
   Source_bitrate=1;
   Throughput(i) = ((length(dataInMatrix)-ber)*Source_bitrate)/length(dataInMatrix);

end
```

```
figure(1)
plot(Carrier_frequency,Throughput,'r-o', 'linewidth' ,2.0);
xlabel('Carrier frequency');
xticks(Carrier_frequency)
ylabel('Throughput');
title ('Throughput to carrier frequency');
grid on;
```

Appendix C: Code for Throughput to mmWave Bandwidth

```
%%%%%%%%%%%%%%%%%%%%code %%%%%%%%%%%%%%
clear all
close all
Throughput=[];
v = VideoReader('xylophone.mp4'); % load a video%
D = v.Duration;                 % duration of a video%
framerate=v.FrameRate;          %Number of frames per second
no=v.NumberOfFrames;            % Number of frames%
time=[];
SNRdB=5;                            %Signal to Noise Ratio in dB
SNR=10.^(SNRdB/10);
t=0;
Throughput_final =[];
for i=1:framerate:no
   t=t+1;
   time = [time t];
   for j=1:framerate
   frames=read(v,i);
   frames = imresize(frames,0.3);
   b=rgb2gray(frames);
   m = reshape(dec2bin(typecast(b(:),'uint8'),8).',1,[])'; %bitstream%
   %convert number of bits into a stream%
   MyStr=m';
   N = 1 ; % the size of each block
```

```
    maxN = numel(MyStr);
    ix0 = 1:N:maxN;
    fh = @(X) MyStr(X:min((X+N-1),maxN));
    B = arrayfun(fh,ix0,'un',0);
    matrix = str2double(B); %%%%%%%%%%%% aka m
    x=(2*matrix)-1;
    y=(sqrt(SNR)*x)+randn(1,length(matrix));
    BER_Simulated=length(find((y.*x)<0));
    Source_bitrate=1;
    Throughput(j) = ((length(matrix)-BER_Simulated)*Source_bitrate)/length(matrix);
    end
    Throughput_final = [Throughput_final mean(Throughput)];
end


figure()
plot(time,Throughput_final,'b-s', 'linewidth' ,1.5);
xlabel('time');
ylabel('Through put');
title ('Throughput to time');
grid on;
```

Appendix D: Code for Bit Error rate to the mmWave Carrier Frequency

```
clear all;
close all;clc
M = 4; % Modulation order (alphabet size or number of points in signal constellation)
k = log2(M); % Number of bits per symbol
v = VideoReader('xylophone.mp4'); % load a video%
D = v.Duration;                  % duration of a video%
framerate=v.FrameRate;


frames=read(v,1);                %read all frames in the video
%a=imshow(frames)
b=rgb2gray(frames);
m = reshape(dec2bin(typecast(b(:),'uint8'),8).',1,[])'; %bitstream%
MyStr=m;
N = 1 ; % the size of each block
maxN = numel(MyStr);
ix0 = 1:N:maxN;
fh = @(X) MyStr(X:min((X+N-1),maxN));
B = arrayfun(fh,ix0,'un',0);
% now B{K} holds the K-th block of N bits of S
%convert string to double%
dataIn = str2double(B)'; %%%%%%%%%%%%% aka m
```

```
sps = 1; % Number of samples per symbol (oversampling factor)


% dataIn = randi([0 1],n,1); % Generate vector of binary data
dataInMatrix = reshape(dataIn,length(dataIn)/k,k);
dataSymbolsIn = bi2de(dataInMatrix);
dataMod = qammod(dataSymbolsIn,M,'bin'); % Binary coding with phase offset of
zero
fs = 300;
Carrier_frequency=28:20:128;
BER=[];
for i=1:6
   fc=Carrier_frequency(i);
   y = modulate(dataMod ,fc,fs,'amssb');
   x = demod(y,fc,fs,'amssb');
   EbNo = 10;
   snr = EbNo+10*log10(k)-10*log10(sps);
   receivedSignal = awgn(x,snr,'measured');
   dataSymbolsOut = qamdemod(receivedSignal,M,'bin');
   dataOutMatrix = de2bi(dataSymbolsOut,k);
   dataOut = dataOutMatrix(:); % Return data in column vector
   [numErrors,ber] = biterr(dataIn,dataOut);
   BER(i) = ber;
end
figure(1)
plot(Carrier_frequency,BER,'g-o', 'linewidth' ,2.0);
```

```
xlabel('Carrier frequency');

xticks(Carrier_frequency)

ylabel('BER');

title ('Bit error rate to carrier frequency');

grid on;
```